USING VISIBLE AND NEAR INFRARED DIFFUSE REFLECTANCE SPECTROSCOPY TO CHARACTERIZE AND CLASSIFY SOIL PROFILES

A Thesis

by

KATRINA MARGARETTE WILKE

Submitted to the Office of Graduate Studies of
Texas A&M University
in partial fulfillment of the requirements for the degree of

MASTER OF SCIENCE

August 2010

Major Subject: Soil Science

USING VISIBLE AND NEAR INFRARED DIFFUSE REFLECTANCE SPECTROSCOPY TO CHARACTERIZE AND CLASSIFY SOIL PROFILES

A Thesis

by

KATRINA MARGARETTE WILKE

Submitted to the Office of Graduate Studies of
Texas A&M University
in partial fulfillment of the requirements for the degree of

MASTER OF SCIENCE

Approved by:

Chair of Committee,	Cristine L. S. Morgan
Committee Members,	C. Tom Hallmark
	J. Alex Thomasson
	Yufeng Ge
Head of Department,	David Baltensperger

August 2010

Major Subject: Soil Science

ABSTRACT

Using Visible and Near Infrared Diffuse Reflectance Spectroscopy to Characterize and Classify Soil Profiles. (August 2010)

Katrina Margarette Wilke, B.S., Texas A&M University

Chair of Advisory Committee: Dr. Cristine L.S. Morgan

Visible and near infrared diffuse reflectance spectroscopy (VisNIR-DRS) is a method being investigated for quantifying soil properties and mapping soil profiles. Because a VisNIR-DRS system mounted in a soil penetrometer is now commercially available for scanning soil profiles in situ, methodologies for using scans to map soils and quantify soil properties are needed. The overall goal of this research is to investigate methodologies for collecting and analyzing VisNIR-DRS scans of intact soil profiles to identify soil series. Methodologies tested include scanning at variable versus uniform moistures, using individual versus averaged spectra, boosting an intact spectral library with local samples, and comparing quantitative and categorical classifications of soil series. Thirty-two soil cores from two fields, representing three soil series, were extracted and scanned every 2.5 cm from the soil surface to 1.5 m or to the depth of parent material at variable field moist conditions and at uniform moist condition. Laboratory analyses for clay, sand, and silt were performed on each horizon. Soil series were classified using partial least squares regression (PLS) and linear discriminant analysis (LDA). A Central Texas intact spectral library (n=70 intact cores) was used for

PLS modeling, alone and boosted with the two fields. Because whole-field independent validation was used, relative percent difference (RPD) values were used to compare model performance. Wetting soils to uniform moisture prior to scanning improved prediction accuracy of total clay and RPD improved by 53%. Averaging side-by-side scans of the same soil profile improved prediction accuracy of RPD by 10%. When creating calibration models, boosting a library with local samples improved prediction accuracy of clay content by 80 and 34% for the two fields. Principal component plots provided insight on the spectral similarities between these datasets. Overall, using PLS alone performed the same as LDA at predicting soil series. Most importantly, results of this project reiterate the importance of fully-independent calibration and validation for assessing the true potential of VisNIR-DRS. Using VisNIR-DRS is an effective way for in situ characterization and classification of soil properties.

ACKNOWLEDGEMENTS

I would like to thank my committee chair, Dr. Morgan, and my committee members, Dr. Hallmark, Dr. Thomasson, and Dr. Ge, for their guidance and support throughout the course of this research.

I would also like to think my fellow graduate students, student workers, faculty, and staff for all the work contributed to my research and for making my experience at Texas A&M so enjoyable. My research would not have been completed had it not been for Travis Waiser, from the Texas NRCS Soil Survey, guiding my field selection and core descriptions, and for Leo Rivera and Scott Stanislav helping with my field work while I was recovering from surgery. Much appreciation goes to Brian Edmonson and the other student workers for the tedious task of grinding and preparing soil samples and to Donna Prochaska for allowing me to use her lab for characterizing my soils. I would also like to thank Texas A&M University for the fellowship that supported me while I was pursuing my degree and to the USDA-NRCS for funding my research.

Finally, I want to thank my wonderful husband Steven Wilke for his continuous support and unconditional love throughout this whole process.

TABLE OF CONTENTS

CHAPTER Page

LIST OF FIGURES

LIST OF TABLES

CHAPTER I

INTRODUCTION

The USDA National Resource Conservations Services (NRCS) National Cooperative Soil Survey (NCSS) is a valuable resource for identifying soils and soil locations in a landscape. Current soil mapping tools are not designed to capture soil variability at fine resolutions. A normal NRCS soil map has a scale of 1:24,000 which does not capture variations between or within mapping units at finer scales. Though information on soil properties at fine resolutions would be beneficial to application such as precision agriculture, watershed modeling, and other precision resource management applications, soil sampling at this resolution is currently cost and labor prohibitive. Some techniques can rapidly measure soil characteristics at finer spatial scales; however, tools that provide fine resolution information on soils provide lower quality data. For example, sensors that measure soil apparent electrical conductivity (EC_a) are soil survey tools that can provide non-invasive, real-time measurements of large areas at a meter-scale, but the information collected shows relative difference across the field. Mapping soil EC_a can show where an important soil property varies, but does not provide absolute information. On the other hand, soil coring combined with lab analysis yields high quality information about the soil profile, but at a coarser spatial resolution. For mapping purposes, soil cores are not collected at a fine resolution; therefore soil data must be interpolated and extrapolated for the areas not sampled. Proximal soil sensing using

---

This thesis follows the style of Soil Science Society of America Journal.

visible and near infrared diffuse reflectance spectroscopy (VisNIR-DRS) has the potential to fill the need for providing soil profile characterization faster than traditional soil coring and lab analysis and complements the high-resolution information provided by EC_a.

Recently using VisNIR-DRS has become a popular method for non-destructively and rapidly quantifying soil properties. The formation of a global library by Brown et al., (2005) sparked interest in developing a larger global library and now VisNIR-DRS is one of the cornerstone methods for the GlobalSoilMap.net project (Sanchez et al., 2009). VisNIR-DRS can provide soil property data on a soil profile faster than traditional soil coring methods and complements both laboratory analysis and high resolution information provided by EC_a. Using VisNIR-DRS has been proven to predict soil properties on air-dried, ground samples and intact cores taken into the lab; however, few studies have evaluated spectroscopy's predictability in the field. The optical fiber of a VisNIR spectrometer can now be mounted into a soil penetrometer, which can take spectral measurements of soil profiles (cm vertical increments) at individual locations in a field. A multi-sensor platform that combines high-resolution aerial data collected horizontally using an EC_a sensor and high-resolution profile data using the VisNIR-DRS would be advantageous for soil mapping.

Though VisNIR-DRS on air-dried, ground soils is moving from research labs to practitioner labs, such as the USDA-NRCS NCSS national lab, much more knowledge is needed regarding how well spectroscopy works on intact cores, how VisNIR-DRS will perform when mounted on a penetrometer, and how to best use spectroscopy to map

soils in the field. Field application of VisNIR-DRS requires development in scanning protocol and in the use of statistical techniques to create a desirable end result.

Though methodologies for collecting and using EC_a measurements are fairly well defined (Corwin and Lesch, 2005), VisNIR-DRS methodology on in situ and on intact cores in the spatial context of a field has not been explored. To achieve the ultimate goal of developing a multi-sensor platform for mapping soils, VisNIR-DRS methodologies for mapping soil profiles in the field need to be better defined. The goal of this research is to determine how VisNIR-DRS scans of soil cores can be used to identify soil properties, horizons, and classification at the soil series level, while using soil EC_a to help define the VisNIR-DRS soil sampling strategy. More specifically, this research will address the following questions: 1) When scanning intact soil scores, is prediction accuracy of soil properties affected by whether soil profiles are uniformly moist (field capacity) or variable (during natural wetting or drying phases); 2) How is prediction accuracy of soil properties affected by combining the same lab-measured clay content based on horizons with individual, 2.5-cm thick soil scans; 3) What is the gain in prediction accuracy by boosting an in situ spectral library with local samples of the same soil series; and 4) How do quantitative predictions of soil properties and categorical classification of VisNIR-DRS data compare when classifying soil profiles at the soil series level? The completion of this work will provide guidance for future application of VisNIR-DRS, penetrometer mounted technology as part of a multi-sensor mapping strategy.

CHAPTER II

LITERATURE REVIEW

Bulk Soil Electrical Conductivity

Soil EC_a is a measurement which provides high resolution meter-scale information and is currently used to map the spatial variability of soils across large areas (Corwin and Plant, 2005). Soil EC_a can be collected with a variety of commercially available instruments. The EM38DD (Geonics Ltd., Mississauga, Ontario, CA) is a conductivity meter that provides measurements of soil EC_a, from the surface to approximately 1.5-m deep, but the actual depth of response for a given soil varies with the soil resistivity (Callegary et al., 2007). Soil EC_a is a measure of the ability of the bulk soil to conduct an electrical current. Soil is generally a poor conductor of electrical current; therefore, the EC_a of soil is primarily a function of the conductivity of the moisture-filled pores within the soil (McNeill, 1980). Soil EC_a is influenced by soil moisture content, the amount and composition of clay, soil porosity, concentration of electrolytes, and temperature (McNeill, 1980; Rhoades et al., 1976). In areas where the soils are well drained, and therefore not saline, soil EC_a properties are primarily influenced by the amount of water, amount of clay, and type of clay minerals.

Originally, EM38DD meters were used to map soil salinity in agricultural fields of the Western U.S. (Rhoades et al., 1976; Rhoades et al., 1989; Rhoades and Corwin, 1981; Lesch et al., 1992). As mentioned, in well drained fields with no salinity, EC_a measurements have been shown to respond to soil moisture (Kachanoski et al., 1988; Sheets and Hendrickx et al., 1992; Khakural et al., 1998; Carroll and Oliver, 2005).

Generally soil water storage and soil EC_a have a linear relationship that may or may not deteriorate at higher water contents (Kachanoski et al., 1988; Sheets and Hendrickx, 1995). Soils with higher clay content hold more soil water; therefore, EC_a responds to soil clay content directly and indirectly.

Because soil EC_a can be used in mapping soil water and clay content, it has been used in precision agriculture applications that need maps of soil spatial variability. The depth to the soil substratum (Doolittle et. al., 1994), depth to clay pan (Vitharana et al., 2008), as well as thickness of the loess layer (Mertens et. al., 2008) have also been mapped using EC_a. Because soil EC_a values are correlated to soil water , soil clay, and soil solum thicknesses, along with many associated soil properties, an EC_a map can be used to employ stratified random sampling to select soil or crop sampling locations (Corwin and Lesch 2005; Johnson et al., 2005).

VisNIR Diffuse Reflectance Spectroscopy

Using VisNIR-DRS as a method for non-destructively and rapidly quantifying soil properties of air-dried, ground soils has become popular. The formation of a global library by Brown et al., (2005) has sparked interest in developing a larger global library and now VisNIR-DRS is one of the cornerstone methods being used in the GlobalSoilMap.net project (Sanchez et al., 2009). Though VisNIR-DRS on air-dried, ground soils is moving from research labs to practitioner labs, e.g. the NCSS national laboratory, much more knowledge is needed regarding how well VisNIR-DRS works on intact cores, how VisNIR-DRS performs when mounted on a penetrometer, and how to best use VisNIR-DRS to map soils in the field (Christy, 2008; Bricklemeyer and Brown,

2010). Field application of VisNIR-DRS requires development in scanning protocol, data management, and in the use of statistical techniques to predict soil properties or to classify soil profiles.

The following review briefly summarizes the prediction accuracies of VisNIR-DRS, but it is important to note that it is difficult to adequately compare results in some studies because of the inconsistency in validation techniques. Techniques to create a validation sample can be non-independent, semi-independent, and fully-independent. Non-independent validations include full-cross or hold-one-out validations, and splitting scans from one soil core between the calibration and validation data sets. Semi-independent includes holding out a percentage of the scans to be randomly divided between validation and calibration data sets. Fully independent validation requires an independently made calibration model and a separate data set for validation. Because holding full fields or similar type areas out of a calibration model and using those scans to estimate prediction error is closer to true independence of the validation data, this method will result in the highest prediction error. When evaluating prediction errors, fully-independent validation samples will provide prediction accuracies more likely to be encountered in practical use than semi- and non-independent validation samples. The other aspect which complicates comparisons is some manuscripts only report the r^2 value of the calibration or just the standard error of prediction (SEP) rather than the SEP and the standard deviation of the soil property being predicted. For example, an SEP of 5 % clay has little prediction power if the standard deviation of the population is 10 % clay compared to a standard deviation of 60 %.

To classify a soil series from a soil core, soil properties such as clay content, inorganic carbon, and organic carbon with depth must be known. VisNIR-DRS has been proven effective in predicting all these properties to varying accuracies, because the properties have absorption features based on molecular overtones and vibrations in the 350-2500 nm range. Clay minerals have distinct spectral signatures because of overtones of OH and combinations of H_2O and CO_2 within the soil minerals (Clark, 1999). Silicate clay mineral have been shown to have distinct absorbance features, e.g. kaolinite has two hydroxyl bands near 1400 nm and 2200 nm (Hunt and Salisbury, 1970); smectite has three strong water bands at 1400, 1900, and 2200 nm (Goetz et al, 2001); and illite has hydroxyl bands at 1400 nm and between 2200 and 2600 nm (Hunt and Salisbury, 1970). The active bonds in organic carbon are O-H, C-N, N-H, and C=O groups, which are primarily in the mid infrared region (Malley et al., 2002). The overtones and combinations of the hydroxyl bonds are located in the NIR region. Inorganic carbon consists primarily of the two minerals calcite and dolomite. These minerals have distinct absorption features at 2500 to 2550 nm, 2300 to 2350 nm, 2120 to 2160 nm, 1970 to 2000 nm, and 1850 to 1870 nm (Clark et al., 1990; Hunt and Salisbury 1971; Gaffey 1986). Lagacherie et al. (2008) used continuum removal at 2340 nm to quantify calcium carbonate of 52 soil samples. In VisNIR-DRS measurement of 72 soil cores, the majority of significant wavelengths for calcite were located in the NIR range (> 1600 nm) for air-dried soil samples and for field moist samples also in the visible range (350-600 nm) (Morgan et al. 2009).

On air-dried, ground soils VisNIR-DRS can predict clay content between 75 and 108 g kg^{-1}. Shepherd et al. (2002) predicted clay content of 1000 air-dried, ground samples from East and South Africa with an SEP of 75 g kg^{-1} using semi-independent 70 % holdout and 30 % validation. Islam et al. (2003) predicted clay content of 161 air-dried, ground samples from Australia with an SEP and relative percent difference (RPD) values of 89 g $kg^{-1}$and 1.9, respectively with semi-independent validation. Brown et al. (2005) created a global spectral library from 3768 air-dried, ground soil samples from all 50 states and Europe. This global library could predict clay content with an SEP value of 95 and 108 g kg^{-1} using two regression techniques and semi-independent 70 % holdout and 30 % validation. Waiser et al. (2007) predicted clay content of 82 air-dried, ground samples from Central Texas with an SEP and RPD value of 62 g $kg^{-1}$and 2.32, respectively using semi-independent 70 % holdout and 30 % validation.

Spectroscopy has also been used to predict soil clay content on intact cores in the lab. Chang et al. (2001) used 802 soil samples to create “natural soil cells” and predicted clay content with an RPD and SEP value of 1.71 and 41 g kg^{-1} using 30 % of the data for semi-independent validation. Waiser et al. (2007) compared clay content prediction of 72 Texas soil samples for field-moist in situ, field-moist smeared in situ, air-dried in situ and air-dried ground using 30 % of the data for semi-independent validation. They obtained SEP values of 61 and 41 g kg^{-1} for field-moist and air-dried in situ cores, respectively, and RPD values of 2.36 and 3.51 for field-moist and air-dried in situ cores, respectively. Waiser et al. (2007) showed that prediction accuracy decreased the SEP from 2.0 to 82.0 g kg^{-1} using whole-field holdout validations (fully-independent).

More recently, researchers have begun to investigate how well spectroscopy can predict clay content in the field. Viscarra-Rossel et al. (2009) used an open soil pit to predict the soil properties along the soil profile with non-independent leave-one-out, cross validation. They were able to accurately measure soil color and predicted the clay content in situ with an SEP of 79 g kg^{-1}. The in situ predictions were better than the lab prediction's the lab predictions had an SEP of 83 g kg^{-1} Ben-Dor et al. (2008) used a contact probe dropped down a hole drilled into the ground. Their results were favorable however they did not set aside independent samples for validation.

On air-dried, ground soils, VisNIR-DRS can predict organic carbon between 3.1 and 6.2 g kg^{-1} (Viscarra-Rossel et al., 2006). Using a 30 % semi-independent validation data set, organic carbon has been predicted with an SEP and RPD of 2.0 g kg^{-1} and 4.2, respectively (Chang and Laird, 2002). Organic carbon has also been predicted on intact cores in the lab. Morgan et al. (2009) predicted the soil carbon with an SEP of 5.4 and 4.1 g kg^{-1} for field-moist and air-dried intact soil cores, respectively using a 30 % semi-independent validation data set. Again prediction accuracy decreased the value of the SEP up to 4.5 g kg^{-1} using fully-independent whole-field holdout validation instead of semi-independent random cross validation (Morgan et al., 2009). In the field, Christy (2008) developed an on-the-go spectrometer to measure organic matter of surface soils. Using fully-independent one-field-out methodology, Christy (2008) obtained an SEP of 5.2 g kg^{-1}.

Inorganic carbon from air-dried, ground samples has been predicted with SEP values ranging from 1.1 to 7.3 g kg^{-1}, using 30 % of the data for semi-independent

validation (McCarty et al., 2002; Chang and Laird, 2002; Morgan et al., 2009). Inorganic carbon has also been predicted on intact cores scanned in the lab. Morgan et al. (2009) predicted the soil inorganic carbon with an SEP and RPD of 7.8 and 8.7 g kg^{-1} and 2.23 and 2.02 for air-dried and field-moist intact soil cores, respectively. Using the soils' reaction with HCl as an auxiliary predictor, improved the SEP and RPD of field-moist intact cores to 6.5 g kg^{-1} and 2.70, respectively. Again, prediction accuracy decreased the value of the SEP from 0 to 15.1 g kg^{-1} using fully-independent whole-field holdout validation versus semi-independent random cross validation (Morgan et al., 2009).

While prediction of air-dried, ground lab samples under uniform conditions has been proven effective, field predictions can be problematic because of the wide range of water content, smearing of the soil, field heterogeneity, and geographic extent of calibration models (Waiser et al., 2007; Brown et al., 2006). To address the smearing effect from a penetrometer on prediction accuracy, soil cores were smeared prior to scanning. Smearing cores showed an increase in prediction error for clay, inorganic carbon, and organic carbon (Waiser et al., 2007; Morgan et al., 2009). Water in soil may obscure spectral information because of the O-H bonds at 1400 and 1900 nm which are important spectral signatures of clay minerals (Bricklemeyer et al., 2010). If water heterogeneity does affect prediction accuracy using VisNIR-DRS, wetting cores to uniform moisture content or surveying soils at uniform moisture (field capacity) may help the accuracy. One study has compared the prediction accuracy of both variable field moist cores and uniformly air-dried cores and found that heterogeneous water content did not affect the clay prediction accuracy, but did affect IC and OC prediction accuracy

(Waiser et al., 2007). Wetting samples in the field is more efficient than drying samples and calibrating field prediction models using field samples is necessary (Minasny et al., 2009). This research plans to address the question of whether uniform moisture in intact cores can increase prediction accuracy compared to non-uniform moisture in soil cores.

Construction of large regional and/or global libraries to increase VisNIR-DRS predictability has been promoted (Brown et al., 2005; Shepherd 2002). The formation of a global library by Brown et al., (2005) sparked interest in developing a larger global library and now VisNIR-DRS is one of the cornerstone methods being used in the GlobalSoilMap.net project (Sanchez et al., 2009). Global libraries alone are not sufficient to predict soil properties; global samples boosted with local samples give the best prediction accuracy for clay, IC, and OC (Brown 2007; Sankey et al., 2008).

Statistical Analysis of Spectral Data

Large amounts of data are acquired when using VisNIR-DRS, especially when scanning soil profiles. For every single soil sample scanned, a large amount of non-independent data that describes the spectral properties of that soil sample are collected. To develop prediction models of soil properties using this spectral data, analysis techniques that reduce and/or transform the data are used. Regression techniques, such as multiple linear regressions (MLR), partial least squares (PLS) regression, regression rules, and boosted regression trees (BRT) are data reduction techniques most commonly used to quantitatively predict soil properties. PLS regression is one of the most common analysis technique seen in the soil science literature (Goetz et al., 2001; Dunn et al., 2002; Waiser et al., 2007; Morgan et al., 2009; Viscarra-Rossel et al., 2009). The

majority of work comparing PLS regression to BRT and MLR show that PLS regression performs just as well or better than the other two methods (Brown et al., 2005, Viscarra-Rossel et al., 2007). In Brown et al. (2005), PLS and BRT predictions resulted in SEP values of 95 and 108 g kg^{-1}, 9.0 and 12.07 g kg^{-1}, and 6.2 and 7.1 g kg^{-1} for clay, inorganic carbon, and organic carbon, respectively. Predictions using regression rules, PLS, and BRT resulted in SEP values of 80, 72, and 86 g kg^{-1} for clay and 3.9, 3.5 and 7.6 g kg^{-1} for total carbon, respectively (Minasny and McBratney, 2008).

Spectral data can be analyzed in many different ways with many end results. How the data are analyzed depends on user needs. Individual soil properties can be predicted quantitatively using PLS, as reported for clay, IC, and OC previously or spectral data can be used for categorically classifying soil taxonomic units. One study (Ben-Dor et al., 2008) explored using VisNIR-DRS to taxonomically classify soil profiles in the field. A contact probe was dropped down a drilled hole and the spectral predictions of soil moisture, soil organic matter, soil carbonates, free iron oxides, and specific surface area were used to describe the soil profile. Conventional descriptions, which were prepared according to the U.S. Soil Taxonomy, were also generated at each soil profile (USDA, 1999). The VisNIR-DRS generated descriptions of each soil profile and conventional descriptions were compared and found to be very similar. Differences between the spectral descriptions and conventional descriptions were noted because higher vertical resolution was obtained by the VisNIR-DRS and some soil properties could not be distinguished with the naked eye, but were distinguished by the spectral

data. The results in Ben-Dor et al. (2008) were favorable; however, as stated before, there were no independent samples for validation.

There are two possible approaches to classifying soils taxonomically. One method is similar to that used by Ben Dor et al. (2008), in which soil properties such as total clay, inorganic carbon, and organic carbon are quantified with depth, and the VisNIR-DRS description of soil properties is used for classification. Another approach is to classify soils into taxonomic units by direct classification. Principal components analysis (PCA) and linear discriminant analysis (LDA) are two methods that can be used together to reduce the large amount of spectral data and classify soils into categorical or taxonomical units. Principal component analysis (PCA) is an orthogonal coordinate system that seeks to maximize the variance along its ordinates. Correlated variables are transformed into a smaller number of uncorrelated variables (Martinez 2001). The first PC describes the largest portion of the total variation in the data. A biplot of principal components is an easy way to visualize the similarities and dissimilarities among soil samples (Gower and Hand, 1996). The distribution of the soils within the biplot gives an indication of the variation between soils (Islam et al., 2005).

Linear discriminate analysis is similar to PCA in that it looks for variables which best explain the data; however, LDA attempts to model the differences between classes, whereas PCA does not account for any difference in classes (Martinez 2001). In soils, LDA has been successfully implemented for direct classification of soil properties, but use of LDA is not common. For example, spectral data on 149 Brazilian soils were collected using laser induced breakdown spectroscopy (LIBS). These soils were

classified to soil order using LDA with a 90 and 72 % classification rate for the independent validation and cross-validation data, respectively (Pontes et al., 2009). In another application, concentrations of hydrocarbons in soil have been classified with a 100 % exact match using spectral data collected on 220 sands with a mass spectrometer (Pavon et al., 2003). This research plans to test how well LDA can classify soils into soil units such as series and horizons.

CHAPTER III

MATERIALS AND METHODS

Site Selection and Soil Coring

Two agricultural fields in Central Texas were chosen based on the heterogeneity and similarity of soil series located in these fields. Both fields were mapped as a complex of two soils series that cannot be shown separately on the NRCS Soil Survey map (Soil Survey Staff, 2008). Each area of a complex contains some of each of the two or more dominant soils, and the pattern and relative proportions are about the same in all areas. Field 100, located in Milam County near Thorndale, TX, 30°36′45″N 97°12′16″W, is approximately 24 ha, and was under a corn (*Zea mays* (L.)) and wheat *(Triticumaestivum* (L.)) rotation. Field 200, located in Lee County near Lincoln, TX, 30° 17′ 15″ N 96° 57′ 48″ W, is approximately 17 ha, and was primarily under continuous corn. The soil series mapped in the fields are Burleson, Wilson, and Davilla, where Burleson is only located in Field 100 (Soil Survey Staff, 2008). Burleson is a fine, smectitic, thermic Udic Haplustert located on Pleistocene age terraces of clayey alluvium; further, it is a Veritsol with either clay loam or clay surface and clay subsoil. Wilson is a fine, smectitic, thermic Oxyaquic Vertic Haplustalf located on terraces or remnant uplands with clayey alluvium parent material of Quaternary age. This Alfisol has a fine particle size class (>35 % clay weighted average, for the first 50 cm of the argillic horizon). Davilla is a fine-loamy, siliceous, superactive, thermic Udic Haplustalf located on Pleistocene age terraces of loamy alluvium. Davilla is also an Alfisol, but has

a fine-loamy particle size class (<35 % clay weighted average, for the first 50 cm of the argillic horizon).

Before obtaining soil cores, 10-m resolution maps of elevation and EC_a were created for each field to provide information for directed sampling (Fig. 3.1 and 3.2). Bulk soil electrical conductivity was measured using an EM38DD (Geonics Ltd., Mississauga, Ontario, CA) landscape survey sensor and a R7/R8 dual frequency GPS (Trimble, Sunnyvale, CA) with a base station and rover antenna (± 2 cm vertical accuracy). The EM38DD was mounted to a wooden sled and pulled behind an ATV while the GPS rover antenna was attached to the top of the ATV. Before each survey, the EM38DD was calibrated according to manufacturer instructions. During each survey the EM38DD was monitored for drift (Sudduth et al., 1995) and kept covered to protect from direct sunlight (Abdu et al., 2007). Ten-meter wide transects were driven while logging all data at 1-s intervals, at a 20 to 30 km hr^{-1} traveling speed.

The EC_a map was used to select locations for obtaining soil cores, and subsequent VisNIR-DRS analysis. Each field was partitioned into four EC_a zones using fuzzy k-means (R Development Core Team, 2004). Four points were randomly located in each EC_a zone. If a sampling location was less than 10 m from a boundary with another EC_a zone, the sampling location was moved so it would be 10 m from the boundary. A total of 32 sampling sites were chosen to collect soil cores with 16 cores in each field (Fig. 3.1 and 3.2). The soil cores were collected with a truck-mounted Giddings hydraulic soil probe in August and September 2008, after harvesting. Soil cores were collected using a metal tube with a 6.0-cm (2 3/8-inch) diameter by 122-cm

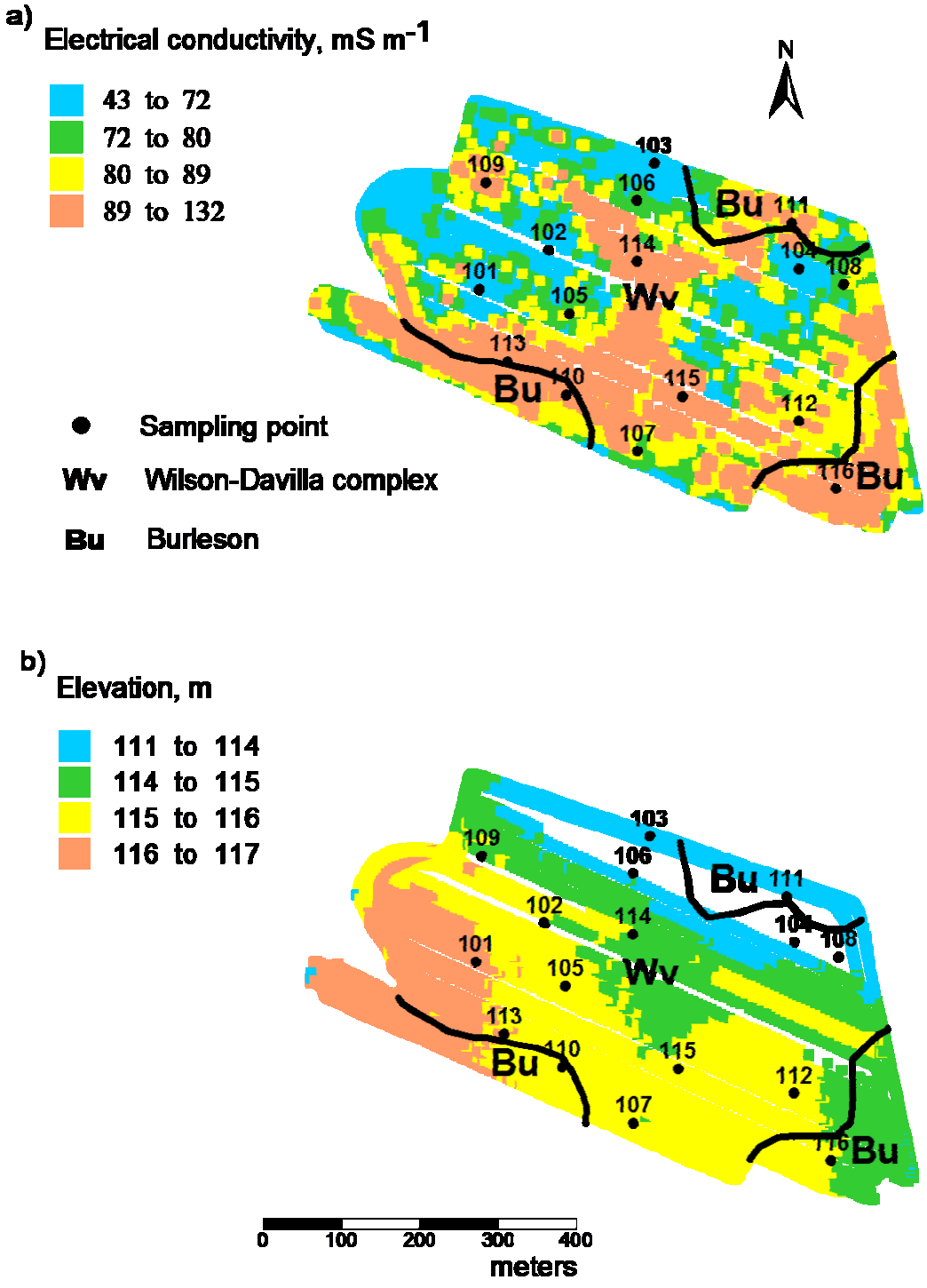

Fig. 3.1. Map of a) four soil apparent electrical conductivity zones and b) elevation with soil series and sampling points for Field 100.

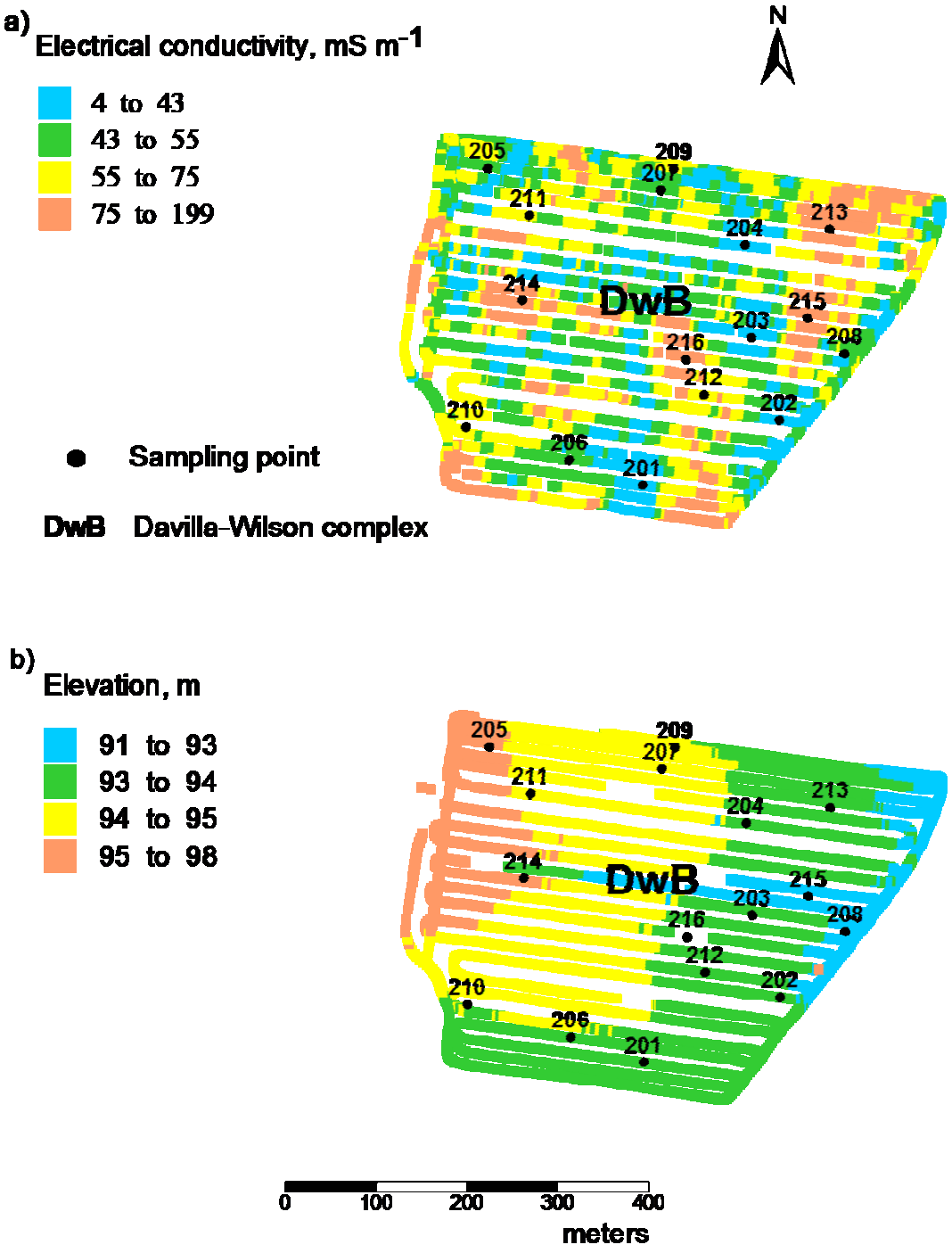

Fig. 3.2. Map of a) four soil apparent electrical conductivity zones and b) elevation with soil series and sampling points for Field 200.

(48-inch) long plastic sleeve. Each core was obtained to 120 cm depth or the depth that the parent material inhibited coring. In Field 200, the parent material was shallow, approximately 50 cm deep, for five of the cores. After extraction, the cores and the hole from which the core was retracted were measured to assess compaction. The soil cores were stored in an ice chest for transport to the lab then in a walk-in cooler at 6.7°C (44°F) for one week prior to scanning.

VisNIR-DRS Scanning and Spectral Processing

The soil cores were transferred from the cooler to the lab and allowed to equilibrate to room temperature prior to scanning. Soil cores were cut in half, lengthwise, using a utility knife to cut the plastic sleeve and a piano wire to cut the soil cores. One-half of each core was used for scanning. A wire grid was used to identify two columns and multiple rows (each row was 2.5-cm thick) on the intact soil core. A schematic of the scanning methodology can be seen in Fig. 3.3. An ASD AgriSpec VisNIR spectrometer (Analytical Spectral Devices, Boulder, CO), with a spectral range of 350-2500 nm, was used to scan the soil cores, using a contact probe containing a halogen white light source within. A white reference Spectralon panel was used prior to scanning each core to set reflectance to 100%. Each row within a column was scanned twice, with a 90º rotation of the contact probe between scans. The soil cores were then wet with distilled water to a uniform wetness and scanned again after equilibrating for 24 hours. Due to processing error, only 11 cores from Field 100 were scanned at uniformly moist conditions.

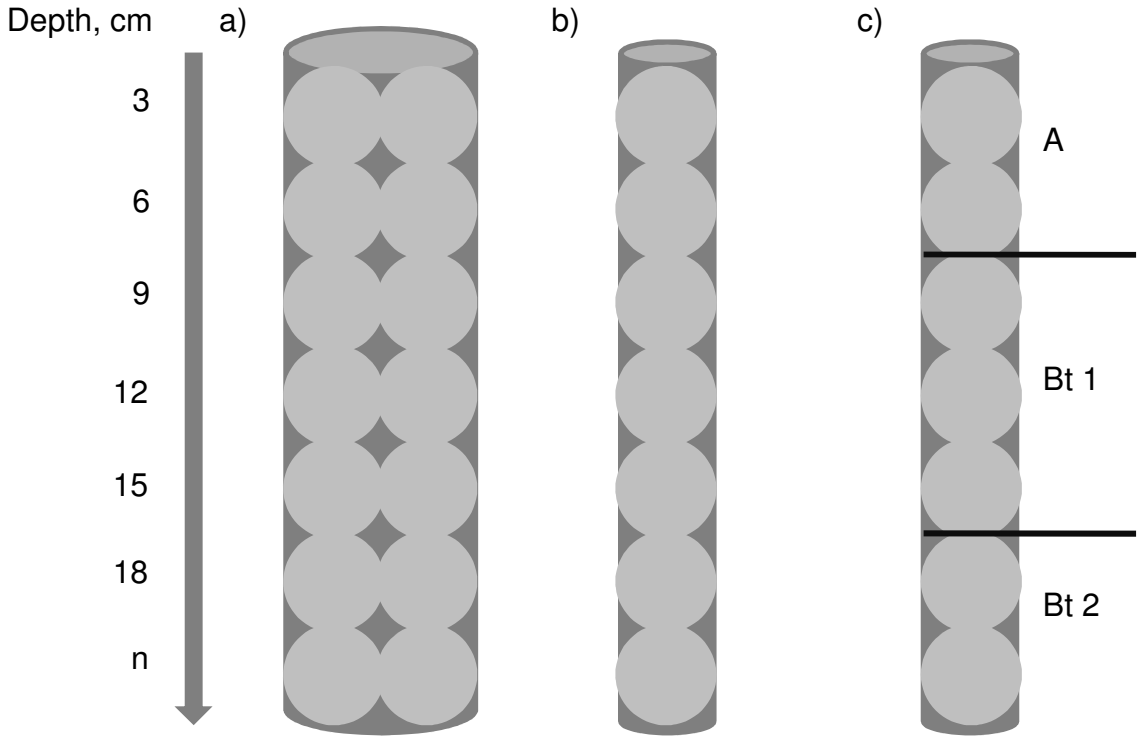

Fig. 3.3. The three pretreatments of the VisNIR-DRS data for creating calibration models using a) all the spectral data individually (n=1422), b) average of VisNIR-DRS data from side-by-side scans (n=711), and c) average of the VisNIR-DRS data within a soil horizon (n=131).

Before analysis, the collected raw spectral data were pretreated by splicing, averaging, and taking the 1st and 2nd derivatives of the reflectance. The spectral data were spliced to produce seamless spectra where the three detectors overlapped across the wavelength spectra. Results of the two replicate scans at 0° and 90° were averaged. Cores were rescanned where the standard deviation of the two replicate scans was greater than 0.50. The mean of the reflectance was calculated at 10-nm intervals (350-2500 nm). A cubic smoothing spline implemented in the R "smooth spline" function (R Development Core Team, 2004) was then fit to each raw spectral curve following the methods of Brown et al. (2006) and Waiser et al. (2007). The 1st derivatives, which were used for model predictions, were then calculated from the reflectance data to reduce albedo.

Sampling for Lab Analysis and Classification

After scanning, horizon depths and soil properties of each core were identified according to NRCS field description. To accurately classify the soil cores into the series each core was first described according to the Soil Taxonomy guide book (USDA, 1999). Both halves of the soil cores were combined by horizon and each horizon was allowed to air dry before analysis. The soil sample was then ground and passed through a 2-mm sieve for particle size distribution analysis and fine ground for total and inorganic carbon analysis. Particle size distribution was determined in the laboratory using the pipette method (Steele and Bradfield, 1934; Kilmer and Alexander, 1949). Total carbon was measured using the dry combustion method (Soil Survey Staff, 1996 and Nelson and Sommers, 1982) and inorganic C was measured using the modified

pressure calcimeter method (Sherrod et al., 2002). Organic C was calculated by subtracting the inorganic carbon from the total carbon (Soil Survey Staff, 1996).

After lab analysis, the measured laboratory data were used to correct the soil series classification. Following direction from the NRCS soil scientist, soil cores from Field 100 were classified according to the texture of the A horizon and soil cores from Field 200 were classified according to the particle class size (Waiser, T. personal communication, 2009). In Field 100, soil cores with a texture of fine sandy loam, loam, and clay loam for the A horizon were classified as a Davilla, Wilson, and Burleson, respectively while in Field 200, soil cores with a particle class size of fine and fine-loamy were classified as Wilson and Davilla series, respectively.

PLS Spectral Analysis

Partial least square regression models were calibrated and validated using both semi-independent and fully-independent techniques. Semi-independent validation was performed by randomly selecting 70 % of the soil cores for the calibration model while the remaining 30 % were used to validate the model. Complete soil cores were randomly selected so that any single core was not split between the calibration and validation datasets. Fully-independent validation was performed by creating the calibration models using whole-field holdouts. Specifically a whole-field holdout refers to using Field 100, Field 200, or a completely independent spectral library for calibration and then validating the model with the remaining cores. Models were built using only the calibration data set, with the first derivative, 10-nm averaged spectral data. The

prediction model was built using 1/25th cross validation PLS regression in Unscrambler 9.0 (CAMO Tech, Woodbridge, NJ).

All calibration models were validated and compared quantitatively using four metrics. The coefficient of determination (R^2), standard error of prediction (SEP), relative percent difference (RPD), and bias were calculated to compare the accuracy of the different PLS models. Statistical formulas to calculate SEP, RPD and bias follow Gauch et al. (2003), Brown et al (2005), Chang et al. (2002) and Waiser et al. (2007).

Because the laboratory measurements of soil properties were performed by horizon and the VisNIR-DRS scans were collected every 2.5 cm along the soil core, three options were explored for developing calibration models and four methods were used for estimating prediction accuracy. All three methods for calibration were based on semi-independent validation. Given that horizon-based laboratory measurements of soil properties are common practices in soil description and mapping, and a benefit of VisNIR-DRS in soils is a fine vertical resolution of soil information, the methodology and results for combing data prior to calibrating a model was explored. The first calibration model used all the spectral data (1 spectrum is the average of two 90^{o}scans) matched individually with lab clay data, (n=1422; Fig. 3.3a). The second calibration model used the mean of side-by-side scans matched to the lab clay data (n=711; Fig. 3.3b). This second option explores any improvement in accuracy that might be available by collecting a second profile scan. The third calibration model averaged (mean) all the spectral scans within a soil horizon, using the core descriptions to identify horizon boundaries, (n=131; Fig. 3.3c). Note that this third estimation requires prior knowledge

of the soil horizons, hence some sort of field description. Finally a fourth estimation of prediction accuracy was made by averaging (mean) the clay content predictions of the second calibration model by horizon, and then comparing those predictions to actual clay content measured by horizon. In essence, the last two options both compare prediction accuracy at the same scale (by horizon). However, the third option combines spectral data by horizon before calibration and the fourth combines spectral predictions by horizon after validation.

Prediction accuracy of clay content using the spectral data from variable and uniform soil moisture was compared for these four models, thereby creating a total of eight models for comparison. The prediction accuracies of all eight models were compared to determine the best model to use for classifying soil cores into series. Even though moisture measurements were not taken for both fields prior to collecting the soil core, Field 100 was much drier than Field 200. In addition to the eight semi-independent models, two side-by-side averaged spectra calibration models were created using whole-field out validation techniques to compare how the variable soil moisture between the two fields affects prediction accuracy.

Finally, to test the predictability of a previously collected in situ VisNIR-DRS library, total clay was predicted using the data set from Waiser et al. (2007). This Central Texas data set consists of 70 cores from 6 fields. Summary statistics for Field 100, Field 200, and the Central Texas data are in Table 3.1. The Central Texas data set was used alone, boosted with Field 100, and boosted with Field 200, to create three calibration

Table 3.1. Soil property summary statistics for Field 100, Field 200, and the Central Texas data set.

Soil property	Mean	SD†	Max.	Min.	Skew	Kurtosis
	----------g kg^{-1}----------					
Field 100 n= 16						
Clay	274.7	59.6	405.7	123.0	-0.87	0.41
Sand	381.6	114.8	770.1	219.9	1.55	2.53
Silt	343.7	78.7	454.4	79.9	-2.13	4.83
Field 200 n=16						
Clay	304.4	115.8	470.1	66.5	-0.81	-0.59
Sand	443.0	147.2	793.8	225.8	0.82	-0.27
Silt	252.5	64.9	388.7	137.1	0.34	-0.92
Field 100 and 200 calibration samples, n = 18						
Clay	313.9	98.2	468.3	69.1	-0.70	-0.23
Sand	398.8	137.3	793.8	229.3	-0.98	-0.15
Silt	287.3	85.3	454.4	79.9	-0.02	-0.63
Field 100 and 200 validation samples, n= 9						
Clay	304.5	100.5	470.2	66.5	-0.80	-0.17
Sand	387.4	147.0	776.3	219.9	1.21	0.75
Silt	308.7	80.3	399.0	147.4	-0.79	-0.91
Waiser et al. (2007) n=71						
Clay	259.5	140.8	578.0	120.0	0.10	-0.60
Sand	481.9	243.5	965.0	500.0	0.30	-0.13
Silt	258.6	130.0	617.0	220.0	-0.13	-0.97
IC‡	16.3	21.8	109.4	0.0	1.60	2.40
OC§	10.6	10.4	55.9	0.0	1.80	3.40

†standard deviation
‡inorganic carbon
§organic carbon

models for clay content. Validation data for the three models were Field 100 and 200, when they were not used in the calibration.

Classifying Soil Series Using PLS

To quantitatively classify soil series using VisNIR-DRS, Fields 100 and 200 were classified into soil series by using PLS. Soil properties were predicted using the uniformly moist side-by-side averaged spectra for PLS model building. Calibration models for clay, sand, and silt were developed using both semi- and fully-independent data sets. The semi-independent models used 70 % of the soil cores from both field to create the calibration model and the remaining 30 % to validate the models. The fully-independent sets used the Central Texas data set boosted with Field 100 or 200, depending on the field being predicted. To base soil series classification on quantitative PLS prediction, texture of the surface horizon and the amount of clay in the particle class size were calculated using the predicted clay, sand, and silt contents.

Classifying Soil Series Using LDA

To categorically classify soil cores using VisNIR-DRS and to bypass the PLS modeling with a more hands off approach, LDA was used to directly classify soil horizons and series on the uniformly moist side-by-side averaged spectra. To initially evaluate the potential of LDA, principal component plots were created to visually assess the spectral distinctness between the horizons and series (Islam et al., 2005). The first three principal components of the first derivatives of the spectral data were created for total clay, soil horizons (A and B) and the soil series (Wilson, Davilla, and Burleson) using the “prcomp” function in R. For LDA analysis the first seven principal

components, were selected because they explained 84 % of the spectral variability of each series or horizon being classified. Using the "lda" function in R, the soil series was classified for each soil core. For LDA training, two sets of training data were used, one was the semi-independent calibration and the other was the fully-independent calibration. The fully-independent model used either Field 100 or 200, depending on the field being predicted. The Central Texas data set was not used for training because the soil series in this library do not match those of Field 100 and 200.

Once the models were trained, soil series were classified for each side-by-side averaged spectrum at every 2.5 cm. The final predicted series for each soil core was chosen as the series classified over 50 % of the time. The kappa coefficient of agreement, which measures the amount of agreement between the actual and LDA predicted classifications, was calculated to compare the accuracy of the different LDA models (Brown et al., 2006). A kappa coefficient of one means there is an almost perfect agreement.

Classifying Soil Series Using LDA Plus PLS

Because using LDA to classify soil series is unreliable, a more guided approach of classifying series was used. Using the "lda" function in R, horizons within each soil core were directly classified as A or B horizons. For LDA training, two sets of training data were used, one was the semi-independent calibration and the other was the fully-independent calibration. The fully-independent model used either Field 100 or 200, depending on the field being predicted. The texture of the A horizon and the particle size

class of the B horizon were then calculated by using the PLS predicted clay, sand, and silt contents.

CHAPTER IV

RESULTS

Soil Series Classification

According to the EM38DD and elevation surveys conducted, Field 100 and Field 200 had EC_a values of 43 to 132 and 4 to 199 mS m^{-1}, respectively and elevations of 111.37 to 116.22 and 91.31 to 98.02 m, respectively (Fig. 3.1 and 3.2). Field 200 had a broader range of EC_a values across the field, and in the highest EC_a zone, all four cores were darker and higher in clay content than the other soil cores. Both Field 100 and 200 had similar changes in elevation across the field. Some short variation in EC_a was seen across both fields, which could be associated with gilgai.

To demonstrate the difficulty in classifying soil cores between Wilson and Davilla, the soil cores sampled for this project were classified three times, each resulting in different outcomes. The cores were classified first according to soil survey maps, second by field descriptions of the actual core, and finally using lab analysis. According to the soil survey map and locations where the soil cores were taken, three soil cores from Field 100 should have been Burleson and the rest from Field 100 and Field 200 should have either been Wilson or Davilla (Fig. 3.1 and 3.2). Based solely on field descriptions, four cores were classified as Davilla and twelve as Wilson in Field 100 and ten as Davilla and six as Wilson in Field 200. However, using the lab particle size analysis, the cores were reassigned to a different series—six Davilla, nine Wilson, and one Burleson series in Field 100 and six Davilla and ten Wilson in Field 200. Table 4.1

Table 4.1. Summary of the NRCS series classification using the lab measured clay content by both the texture of the A horizon and the particle control section. Highlighted sections indicate how the soil was classified by NRCS soil scientist protocol.

Cores	NRCS Series Classification			
	Particle Size Class Series	Particle Size Class Clay Percent	A Horizon Texture Series	A Horizon Texture
101	Davilla	28.3	Davilla	Fine sandy loam
102	Davilla	26.9	Wilson	Loam
103	Davilla	29.3	Davilla	Fine sandy loam
104	Davilla	27.8	Davilla	Fine sandy loam
105	Davilla	29.1	Davilla	Fine sandy loam
106	Davilla	31.4	Davilla	Fine sandy loam
107	Davilla	27.2	Wilson	Loam
108	Davilla	31.3	Wilson	Loam
109	Davilla	31.5	Wilson	Loam
110	Davilla	30.8	Wilson	Loam
111	Davilla	24.8	Wilson	Loam
112	Davilla	25.5	Davilla	Fine sandy loam
113	Davilla	34.1	Burleson	Clay loam
114	Davilla	34.0	Wilson	Loam
115	Davilla	33.2	Wilson	Loam
116	Davilla	31.1	Wilson	Loam
201	Wilson	42.2	Davilla	Fine sandy loam
202	Wilson	46.5	Davilla	Fine sandy loam
203	Davilla	31.6	Davilla	Fine sandy loam
204	Davilla	33.9	Davilla	Fine sandy loam
205	Wilson	42.2	Davilla	Fine sandy loam
206	Davilla	30.8	Davilla	Fine sandy loam
207	Wilson	38.6	Davilla	Fine sandy loam
208	Davilla	21.3	Wilson	Loam
209	Davilla	33.9	Davilla	Fine sandy loam
210	Davilla	29.6	Davilla	Fine sandy loam
211	Wilson	36.1	Davilla	Fine sandy loam
212	Wilson	37.9	Wilson	Loam
213	Wilson	41.3	Wilson	Loam
214	Wilson	39.3	Davilla	Fine sandy loam
215	Wilson	41.9	Wilson	Loam
216	Wilson	37.1	Wilson	Loam

summarizes the final soil core classifications according to the NRCS soil scientist protocol for both Field 100 and 200.

Effect of Uniform and Variable Soil Moisture

To determine if the prediction accuracy of a PLS model for soil clay can be improved with scanning soil cores at uniform soil moisture; prediction models were built using both variable and uniform moisture content. According to the results of the semi-independent models, wetting soils to uniform moisture prior to scanning slightly improved predictions (Table 4.2). In general by using scans of uniform soil moisture, the r^2 increased and the RPD improved by 6 to 13 %. For all four models, the bias increased with uniformly moist scans. It should be noted that the standard deviations between the uniform and variable moistures are different for Field 100 because 5 cores were processed before scanning them at uniform moisture.

As expected, fully-independent, whole-field, models yielded poorer predictions than the semi-independent models; however, these results provide more evidence that uniform moisture improves prediction accuracy (Table 4.3). The fully-independent predictions of clay improved RPD values by 44 and 64 % in Field 100 and 200, respectively. The sand predictions were less conclusive. Soil cores in Field 200 were wetter than the soil cores in Field 100 because a light rain occurred one week prior to sampling Field 200. The average reflectance of both the uniformly moist and variable moist scans of all the soil cores had distinct peaks at 1400, 1900, and 2100 nm (Fig. 4.1). Soil cores at field moisture had higher reflectance than the uniformly moist soil cores

Table 4.2. Prediction of total clay content using the 1st derivative of VisNIR reflectance and the four methods used for estimating prediction accuracy of the PLS semi-independent calibration models.

	Individual Spectra	Side-by-side averaged spectra	Horizon averaged spectra	Horizon averaged clay predictions
Variable Moisture				
r^2	0.76	0.77	0.86	0.85
SEP†, g kg^{-1}	49.2	48.9	42.3	40.9
RPD†	2.00	2.02	2.43	2.52
Bias, g kg^{-1}	-9.00	-10.9	-18.6	-7.90
PCs†	6	7	6	7
Uniform Moisture				
r^2	0.76	0.80	0.89	0.89
SEP, g kg^{-1}	48.4	47.0	40.4	36.7
RPD	1.92	2.14	2.59	2.85
Bias, g kg^{-1}	-16.92	-13.7	-20.9	-12.8
PCs	5	5	5	5

† SEP, RPD, and PCs are standard error of prediction, residual prediction deviation, and principal components, respectively.

Table 4.3. Prediction accuracy of clay content using fully-independent, whole-field holdouts under variable and uniformly moist soil conditions for the side-by-side averaged spectral data.

Soil property	r^2	SEP†, g kg^{-1}	RPD†	Bias, g kg^{-1}	PCs†
		Variable Moisture			
Field 100 validation, n=16					
Clay	0.54	59.3	1.07	40.6	5
Sand	0.19	108.0	1.00	-42.9	8
Silt	0.04	78.8	0.86	-6.7	9
Field 200 validation, n=16					
Clay	0.53	137.3	0.85	-111.1	4
Sand	0.64	123.3	1.20	28.9	10
Silt	0.56	107.4	0.61	52.4	10
		Uniform Moisture			
Field 100 validation, n=11					
Clay	0.60	38.7	1.54	4.5	5
Sand	0.65	94.01	1.23	59.3	11
Silt	0.18	94.5	0.83	-61.4	8
Field 200 validation, n=16					
Clay	0.53	83.4	1.39	-24.7	11
Sand	0.49	132.8	1.12	14.60	7
Silt	0.01	261.18	0.25	195.5	11

† SEP, RPD, and PCs are standard error of prediction, residual prediction deviation, and principal components, respectively.

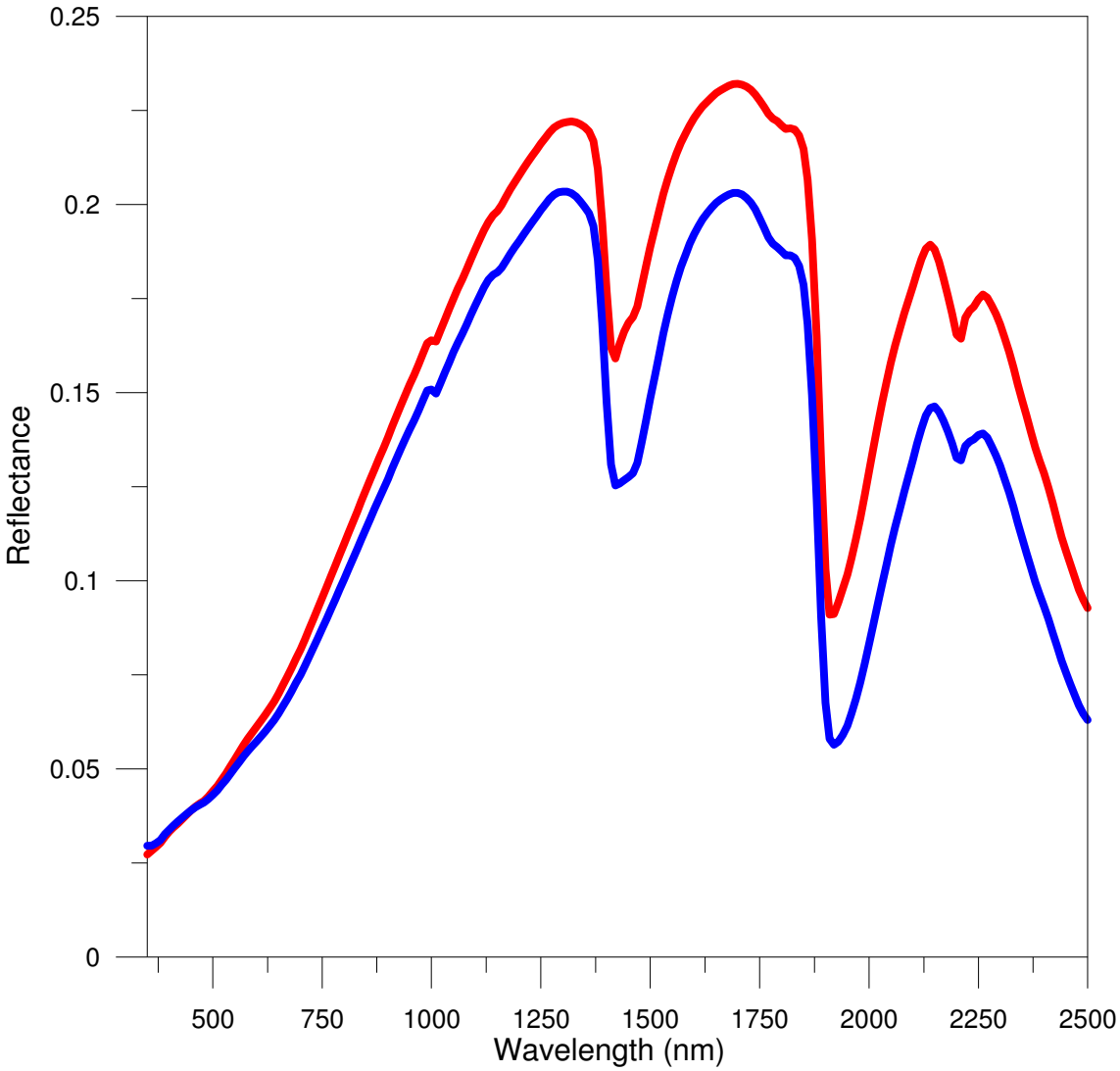

Fig. 4.1. Average of the reflectance of the spectral scans at field moisture (red) and uniform moisture (blue) for the cores in Field 100 and 200.

(Fig. 4.1). Because uniform moisture showed an increase in predictability, the rest of the analyses were performed on the uniformly moist spectral data.

Prediction Accuracy from Averaging Multiple Scans

Overall, the estimated prediction accuracy of the three PLS clay prediction models built using the individual spectra data, the side-by-side averaged spectra, and the horizon averaged spectra all showed improvement with averaging (Table 4.2). Using individual spectra without averaging to predict clay yielded poorest prediction accuracy (Fig. 4.2a). To simulate techniques available used with a VisNIR-DRS mounted penetrometer, where horizon depths are unknown but the penetrometer collects two sets of scans for a soil profile, the side-by-side averaged spectra improved clay prediction by 1.5 g $kg^{-1}$and the RPD to 2.14 (Fig. 4.2b). Averaging the spectral data of each soil horizon before predicting clay content improved the prediction accuracy by 7.4 g $kg^{-1}$and the RPD to 2.59 (Fig. 4.2c). Lastly using the side-by-side averaged spectra prediction model (Fig. 4.2b) and averaging the predicted clay content of each horizon provides a more representative presentation of how well the VisNIR-DRS is predicting clay with a bias, SEP, and RPD of -12.8, 36.7 g kg^{-1}, and 2.85 respectively (Fig. 4.2d). Overall, not averaging the spectra by soil horizon before putting the data into a PLS calibration is the practical option because horizon depths will likely not be known when using VisNIR-DRS attached to a penetrometer in the field. However if time allows, the added data from side-by-side scans is useful. The rest of the analyses were performed using the uniformly moist side-by-side averaged spectra.

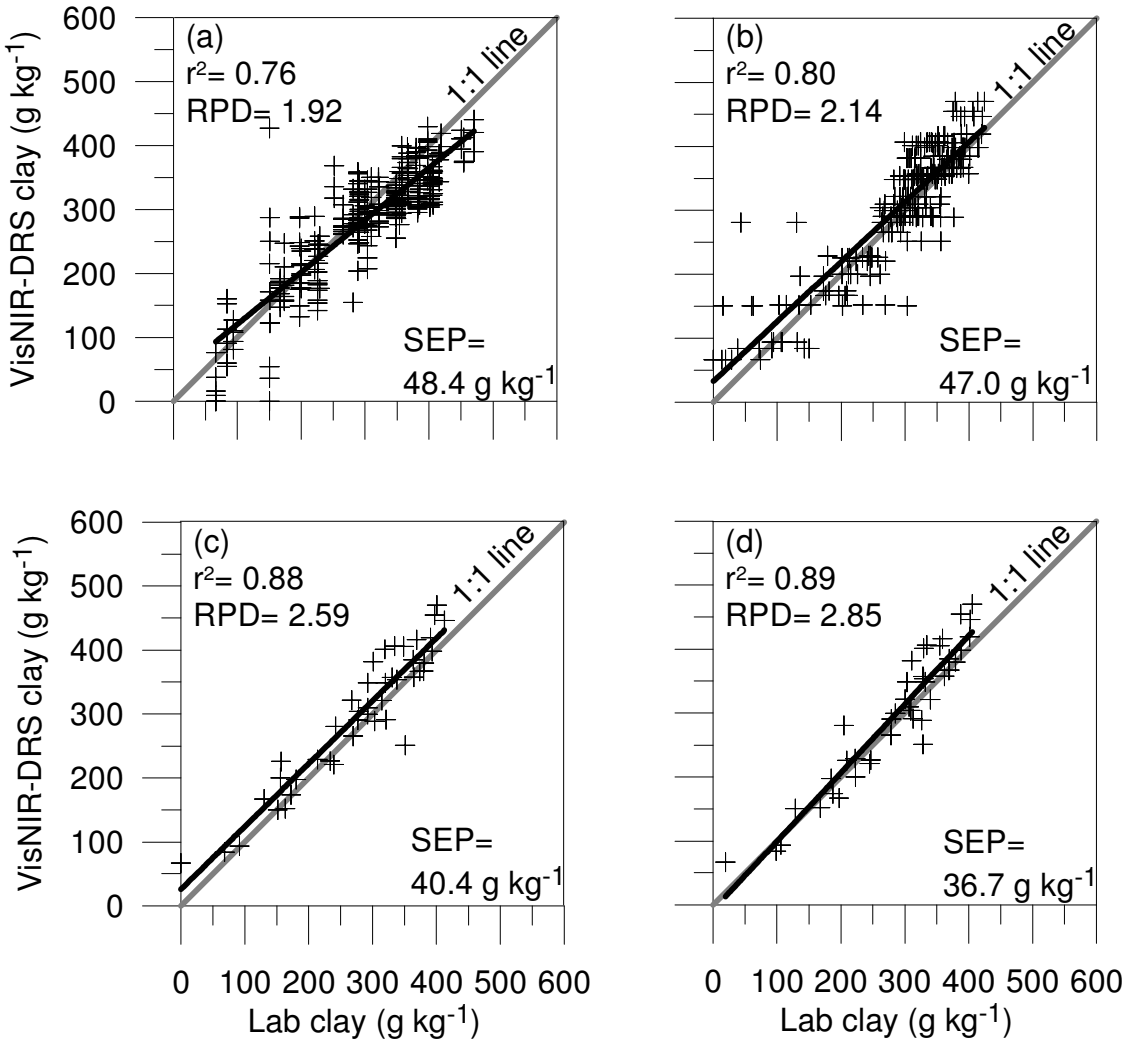

Fig. 4.2. Uniformly moist predicted vs. measured clay content of the validation data for (a) individual spectra, (b) side-by-side averaged spectra, (c) spectra averaged by horizon, and (d) predictions averaged by horizon.

Performance of the Central Texas Spectral Library

Because two small fields mapped as similar soil series provide little variability and a conceptual VisNIR-DRS soil mapping expedition would use a VisNIR-DRS library, 70 cores from the Central Texas data set were used with Field 100 and 200 cores to create three PLS calibration models for clay, sand, and silt. The calibration models were created using the Central Texas data alone, the Central Texas data boosted with Field 100, and the Central Texas data boosted with Field 200. Boosting the Central Texas data set with Field 100 and 200, improved predictions of clay, sand, and silt (Table 4.4). Boosting with Field 100 improved the RPD of clay predictions by 34% and boosting with Field 200 improved the RPD by 80 %. The RPD of sand predictions was improved by 55 and 36 % for Field 100 and 200, respectively. These results indicate that using an in situ library of soil core scans boosted with local samples, which have similar properties as the validation, is a preferable method for characterizing properties of soil cores.

PLS Classification of Soil Series

The soil cores were classified to soil series using PLS-based predictions of sand, silt, and clay and then assigned a series according to both the texture of the A horizon and the particle size class. For comparison purposes, two PLS models were built with the semi-independent data and the fully-independent Central Texas data boosted by the field not being classified. Clay content, predicted using PLS, of one core from each of the three soil series is plotted with depth (Fig. 4.3). By graphing the predicted clay content by depth for each soil core, the Alfisols (Wilson and Davilla) were easy to distinguish

Table 4.4. Prediction accuracy of clay content using fully-independent, whole-field holdout for the uniformly moist side-by-side averaged spectra. Models were created with the Central Texas data alone and boosted with Field 100 or 200 scans.

Soil property	r^2	SEP†, g kg^{-1}	RPD†	Bias, g kg^{-1}	PCs†
Central Texas calibration unboosted					
		Field 100 validation			
Clay	0.57	121.2	0.49	114.3	9
Sand	0.48	119.6	0.96	-86.6	8
Silt	0.43	70.0	1.12	-32.6	7
		Field 200 validation			
Clay	0.55	103.2	1.12	65.9	9
Sand	0.47	137.9	1.06	-14.4	8
Silt	0.53	64.8	1.00	-24.7	7
Central Texas calibration boosted with Field 200					
Clay	0.57	67.7	0.88	53.9	5
Sand	0.56	77.0	1.49	-1.8	8
Silt	0.27	82.6	0.95	-46.6	9
Central Texas calibration boosted with Field 100					
Clay	0.55	78.42	1.50	3.06	9
Sand	0.65	103.9	1.44	-29.9	8
Silt	0.52	68.5	1.63	-4.3	8

† SEP, RPD, and PCs are standard error of prediction, residual prediction deviation, and principal components, respectively.

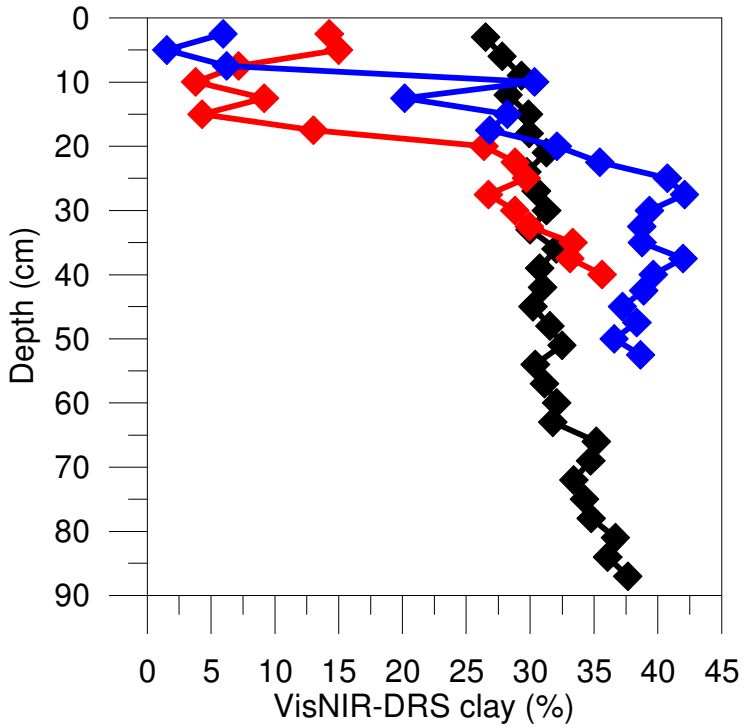

Fig. 4.3. Predicted clay plotted with depth for Wilson series (blue), Davilla series (red) and Burleson series (black) cores.

because of the sharp increase in clay content (Fig. 4.3). The Burleson series (plotted in black, Fig. 4.3) was consistent in clay content throughout.

The A horizon was distinguished from the B horizon by looking for increases in clay. The first 20 spectra (2.5 cm each) starting at the top of the B horizon were used to calculate the particle size class. Using the semi-independent model to predict both the texture of the A horizon and the particle size class, all cores from Field 100 and 200 were correctly classified to soil series (Table 4.5). Using fully-independent Central Texas boosted model, 19 of the 27 soil cores from Field 100 and 200 were correctly classified to soil series with a kappa coefficient of 0.50 (Table 4.6). Eighty-one percent of Field 200 cores and 55 % of Field 100 cores were classified correctly.

Principal Components Analysis

Principal components plots based on clay content show that Field 100 and the Central Texas data soils are spectrally similar, while Field 200 soils have similar and dissimilar spectral features (Fig. 4.4). The first three principal components with respect to soil horizons A and B show some differentiation by horizon, particularly in the first two principal components (Fig. 4.5). Overall, the three soil series appear to overlap each other and do not clearly differentiate in the principal component plot (Fig. 4.6). The Davilla series spreads across the plot and between the other two series. The spectral properties of Burleson and Wilson aggregate together and are hard to differentiate.

LDA Classification of Soil Series

Linear Discriminant Analysis was performed to bypass the step of developing PLS models to predict texture. The first seven principal components explained 94 % of

Table 4.5. NRCS soil series and the semi-independent PLS based series classification. Series were classified by both the texture of the A horizon and the particle control section. Highlighted sections indicate how the soil was classified by NRCS soil scientist protocol.

Cores	NRCS Series Classification		Predicted Series Classification	
	Particle Size Class	A Horizon Texture	Particle Size Class	A Horizon Texture
107	Davilla	Wilson	Davilla	Wilson
111	Davilla	Wilson	Davilla	Wilson
113	Davilla	Burleson	Davilla	Burleson
114	Davilla	Wilson	Davilla	Wilson
204	Davilla	Davilla	Davilla	Davilla
206	Davilla	Davilla	Davilla	Davilla
207	Wilson	Davilla	Wilson	Davilla
211	Wilson	Davilla	Wilson	Davilla
212	Wilson	Wilson	Wilson	Wilson

Table 4.6. NRCS series and the PLS bases series classification using the fully-independent Central Texas data boosted with Field 100 and 200. Series were classified by both the texture of the A horizon and the particle control section. Highlighted sections indicate how the soil was classified by NRCS Soil Scientist protocol. Series labeled in **bold** were misclassified.

Cores	NRCS Series Classification		Predicted Series Classification	
	Particle Size Class	A Horizon Texture	Particle Size Class	A Horizon Texture
106	Davilla	Davilla	**Wilson**	Davilla
107	Davilla	Wilson	**Wilson**	**Davilla**
108	Davilla	Wilson	**Wilson**	**Davilla**
109	Davilla	Wilson	**Wilson**	**Burleson**
110	Davilla	Wilson	**Wilson**	**Burleson**
111	Davilla	Wilson	Davilla	Wilson
112	Davilla	Davilla	Davilla	Davilla
113	Davilla	Burleson	**Wilson**	Burleson
114	Davilla	Wilson	**Wilson**	**Davilla**
115	Davilla	Wilson	Davilla	Wilson
116	Davilla	Wilson	Wilson	Wilson
201	Wilson	Davilla	**Davilla**	Davilla
202	Wilson	Davilla	Wilson	Davilla
203	Davilla	Davilla	Davilla	Davilla
204	Davilla	Davilla	Davilla	Davilla
205	Wilson	Davilla	**Davilla**	Davilla
206	Davilla	Davilla	Davilla	Davilla
207	Wilson	Davilla	**Davilla**	Davilla
208	Davilla	Wilson	**Davilla**	Wilson
209	Davilla	Davilla	Davilla	Davilla
210	Davilla	Davilla	Davilla	Davilla
211	Wilson	Davilla	Wilson	Davilla
212	Wilson	Wilson	Wilson	**Burleson**
213	Wilson	Wilson	Wilson	**Burleson**
214	Wilson	Davilla	Wilson	**Burleson**
215	Wilson	Wilson	Wilson	**Burleson**
216	Wilson	Wilson	Wilson	**Burleson**

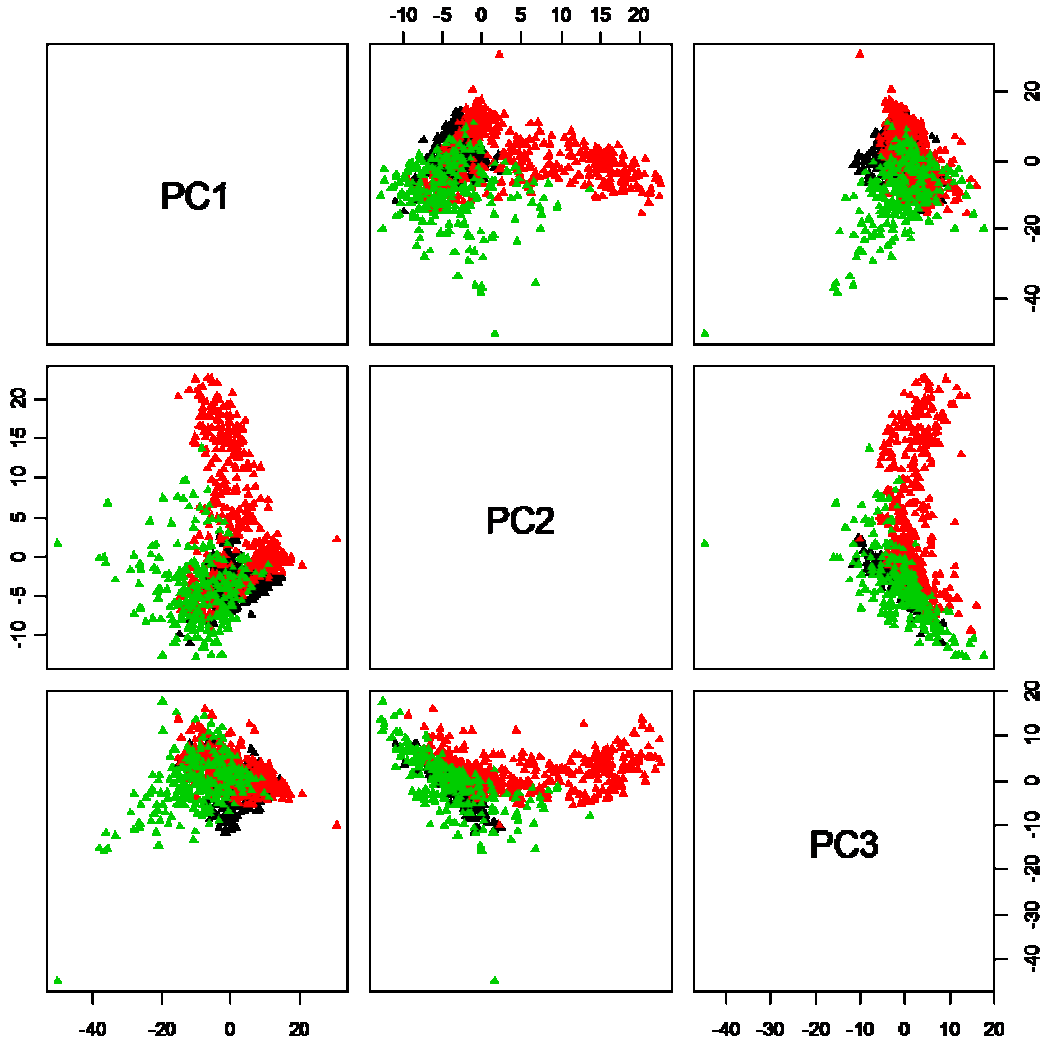

Fig. 4.4. Cluster plot of the first three principal components based on clay for Field 100 (black), Field 200 (red), and the Central Texas data (green) using the first derivatives of the reflectance for uniform moisture. The first three principal components account for 84% of the variability.

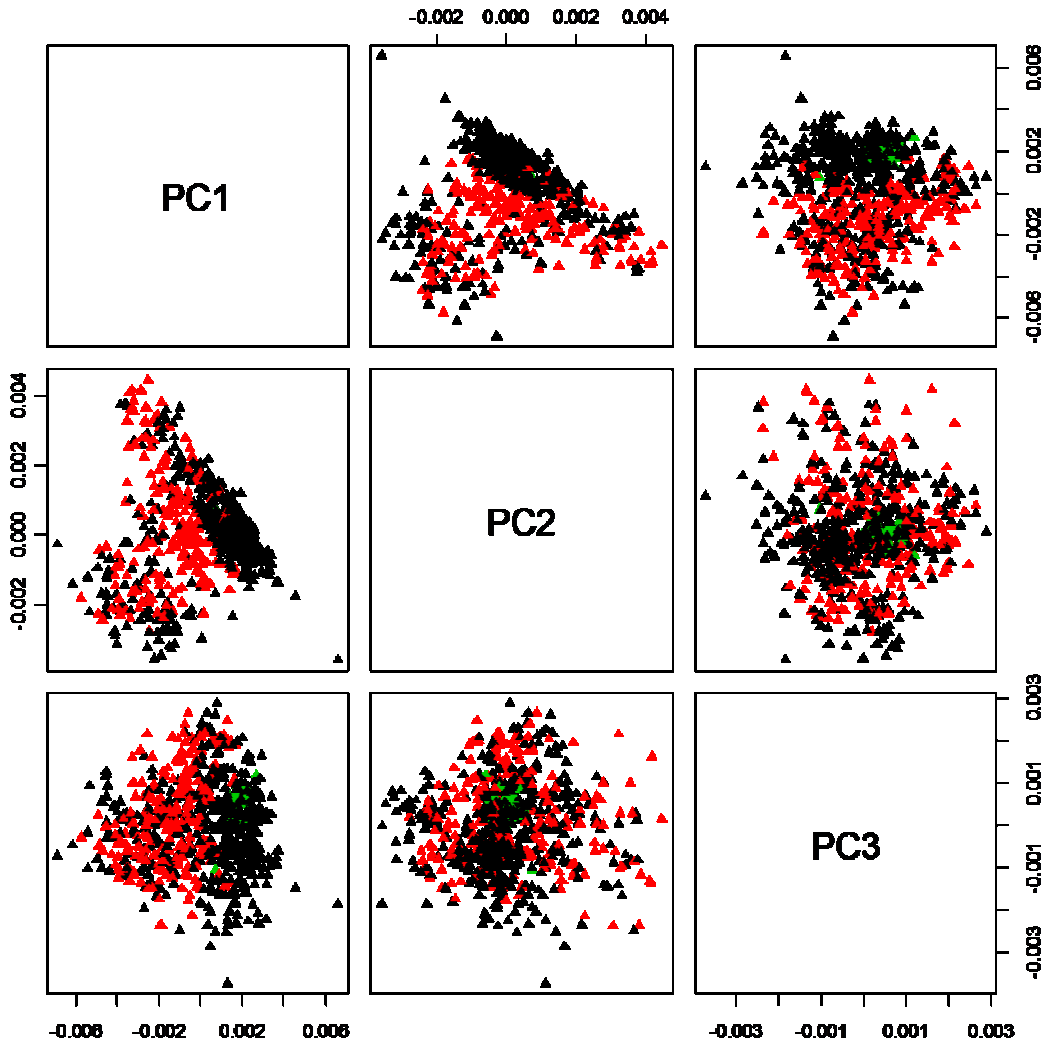

Fig. 4.5. Cluster plot of the first three principal components of the soil series Wilson (red), Davilla (red), and Burleson (green) using the first derivatives of the reflectance for uniform moisture. The first three principal components account for 84% of the variability.

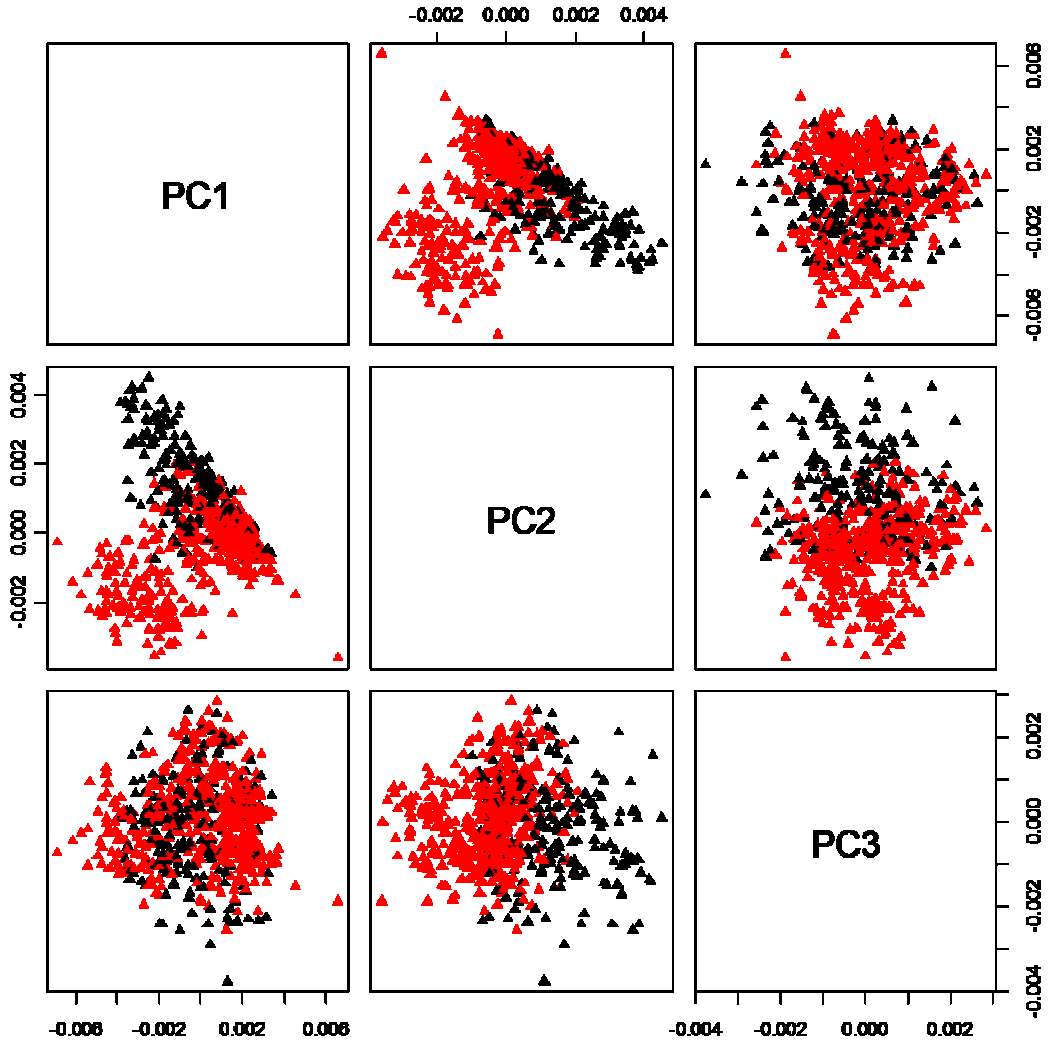

Fig. 4.6. Cluster plot of the first three principal components of the soil horizons A (black) and B (red) using the first derivatives of the reflectance for uniform moisture. The first three principal components account for 84% of the variability.

the spectral variability and were used in LDA to directly classify soil cores into series and to directly classify soil horizons. Using the semi-independent calibration, soil series were classified correctly 78 % of the time; the kappa coefficient was 0.54 (Table 4.7). As expected, LDA performed poorer with fully-independent training, soil series were classified correctly 73 % of the time in Field 100 and 69 % of the time in Field 200; the kappa coefficients were 0.41 and 0.39, respectively (Table 4.7).

LDA Plus PLS Classification of Soil Series

Because direct LDA classification of soil series was so unreliable, a more guided approach that included directly classifying soil horizons first was used. Texture and particle size class were obtained on the LDA-classified horizons to determine soil series. Using the semi-independent training, 70 % of the soil horizons were classified correctly; the kappa coefficient was 0.35. By using both the texture of the A horizon and the particle class size for the LDA horizons, all of the soil cores were correctly classified to soil series (Table 4.7).

The guided LDA approach performed poorer with fully-independent training. Soil horizons of Field 100 and 200 were classified correctly with exact matches of 60 and 81 %, respectively. Field 100 predictions were barely better than a guess hence the kappa coefficient was 0.04. Field 200 performed better with a kappa coefficient of 0.47. By using both the texture of the A horizon and the particle class size for the LDA horizons, 14 of the 27 soil cores were correctly classified to soil series (Table 4.7).

Table 4.7. Summary of the PLS, LDA, and LDA plus PLS series classification. Series labeled in bold were misclassified. Highlighted sections indicate soil cores that were misclassified using all three methods.

Cores	NRCS Series	PLS Series	LDA Series	LDA plus PLS Series
		Semi-independent Calibration		
107	Wilson	Wilson	Wilson	Wilson
111	Wilson	Wilson	Wilson	Wilson
113	Burleson	Burleson	**Wilson**	Burleson
114	Wilson	Wilson	Wilson	Wilson
204	Davilla	Davilla	Davilla	Davilla
206	Davilla	Davilla	Davilla	Davilla
207	Wilson	Wilson	**Davilla**	Wilson
211	Wilson	Wilson	Wilson	Wilson
212	Wilson	Wilson	Wilson	Wilson
		Fully-independent Calibration		
106	Davilla	Davilla	**Wilson**	**Wilson**
107	Wilson	**Davilla**	Wilson	Wilson
108	Wilson	**Davilla**	Wilson	**Davilla**
109	Wilson	**Burleson**	**Davilla**	**Davilla**
110	Wilson	**Burleson**	Wilson	**Burleson**
111	Wilson	Wilson	Wilson	Wilson
112	Davilla	Davilla	Davilla	Davilla
113	Burleson	Burleson	**Wilson**	Burleson
114	Wilson	**Davilla**	Wilson	Wilson
115	Wilson	Wilson	Wilson	**Burleson**
116	Wilson	Wilson	Wilson	**Burleson**
201	Wilson	**Davilla**	**Davilla**	**Davilla**
202	Wilson	Wilson	**Davilla**	**Davilla**
203	Davilla	Davilla	Davilla	Davilla
204	Davilla	Davilla	Davilla	Davilla
205	Wilson	**Davilla**	**Davilla**	**Davilla**
206	Davilla	Davilla	Davilla	Davilla
207	Wilson	**Davilla**	**Davilla**	**Davilla**
208	Davilla	Davilla	**Wilson**	Davilla
209	Davilla	Davilla	Davilla	Davilla
210	Davilla	Davilla	Davilla	Davilla
211	Wilson	Wilson	Wilson	Wilson
212	Wilson	Wilson	Wilson	**Davilla**
213	Wilson	Wilson	Wilson	**Davilla**
214	Wilson	Wilson	Wilson	Wilson
215	Wilson	Wilson	Wilson	Wilson
216	Wilson	Wilson	Wilson	**Davilla**

CHAPTER V

DISCUSSION

1) When scanning intact soil scores, can VisNIR-DRS prediction accuracy be improved by scanning cores that are uniformly moist (i.e. at field capacity) rather than at non-uniform moistures (i.e. during wetting or drying phases)?

Previous studies have shown that soil moisture can negatively affect prediction accuracy when using VisNIR-DRS (Wasier et al., 2007; Minasny et al., 2009; Bricklemeyer et al., 2010). Although the absorption peaks appear to be the same with varying moisture, the shape and height of the peak can be different with varying soil moisture (Minasny 2009). Also, because the distinct absorption peaks for clay minerals are at 1400, 1900, and 2200 nm (Shepherd and Walsh, 2002), and the O-H bonds for water are at 1400 and 1900, soil moisture may obscure spectral information (Bricklemeyer et al., 2009). Plots of the average reflectance for uniform and varying soil moisture of the two fields in this study are consistent with previous studies because the average reflectance of the uniformly moist and variable moist scans both had distinct peaks at 1400, 1900, and 2100 nm (Fig. 4.1). Both moistures had similar spectral shapes; however, the soil cores at field moisture had higher reflectance than the uniformly moist soil cores (Fig. 4.1).

Processing soils (e.g. homogenizing) in the field prior to scanning has been suggested to increase the uniformity of the soil spectra, and thereby improve predictability (Bricklemeyer et al., 2010). Wetting cores to uniform moisture content as an approach to create a more uniform data set, seems more practical than drying cores,

because wetting can be done quickly in the field prior to scanning a soil core sample (Minasny et al., 2009). Waiser et al., (2007) compared the prediction accuracies for clay content of field moist cores with variable water contents to that of air-dried cores. The prediction accuracies of the PLS models of clay content using scans of air-dried cores improved by 20 g kg^{-1} over the PLS models using scans of soil cores with variable water contents (Waiser et al., 2007).

In this study, prediction accuracy of the fully-independent models yielded poorer predictions than the semi-independent models; however more importantly, scans of uniformly moist soils improved the prediction accuracy quite significantly (Table 4.2 and 4.3). This improvement in the fully-independent models is evidence that uniform moisture is very important for creating robust in situ spectral libraries. The semi-independent model did not show improvement in prediction accuracy with different moisture contents. This lack of improvement shows how important it is to have fully-independent validations especially when working with PLS. In the semi-independent model, PLS was compensating for the variable moistures within the field. These results comparing the fully- and semi-independent validation provide further evidence that caution is needed in spectroscopy investigations that use PLS.

The data set used to test the effect of soil moisture is relatively small, 32 cores from 2 fields; consequently, this test has less power than any similar test using more soil cores and fields. Until additional results from other studies are reported, it is suggested instead of wetting soils prior to scanning, soil cores or VisNIR-DRS pentrometer surveys

could be collected when the soil is near field capacity to ensure the soil is near uniform moisture.

2) How does the estimation of prediction accuracy change when spectra from multiple scans are averaged?

Estimates of prediction accuracy are affected depending on how spectral data are combined for both calibration and prediction. Scans are made continuously along a soil profile, and even if several scans are made along one horizon, laboratory analysis was made on the whole horizon. This mismatch in fine-scale (2.5 cm) scanning and coarse-scale (whole horizon) lab analysis creates variability in estimates of prediction accuracy. Scatter in the validation data is present in each horizon; however, it is difficult to tell what the error is and what the true variation in clay content with depth is. The spectrometer is predicting a change in the clay percent with depth, which can be seen as a vertically straight line on the graph because one value on the x-axis (measured clay) is the same for several values on the y-axis (VisNIR-DRS clay) (Fig. 4.2.). Although gradual changes in clay content within an argillic horizon is realistic, it is unclear how to interpret the validation results.

Results of this study show that the extra effort and time required to scan another column along a soil profile, may not be worth the small improvement in prediction accuracy for clay content (11 % improvement in RPD). Previous work on intact cores (Morgan et al., 2009) averaged side-by-side scans and increased RPD prediction accuracy by about 22 and 8 % for inorganic carbon and organic carbon, respectively.

Depending on the scope and time frame of the project, an extra column of scans along a soil profile may be beneficial especially where concentrations (e.g. inorganic carbon or organic carbon) may occur (Morgan et al., 2009). Averaging the scans will increase the quality of the scans when it is not possible to rescan soil samples (e.g. in situ scans).

Averaging all VisNIR spectra by horizon improved the RPD by 17 and 25 % for the horizon averaged spectra and the horizon averaged clay predictions, respectively (Table 4.2). However averaging by horizon is impractical because horizon depths may not be known when using VisNIR-DRS attached to a penetrometer in the field. Because lab measurements were taken by horizon and used in the calibration models, averaging the spectra and the predicted clay content by horizon provides an idea of how well VisNIR-DRS is performing statistically. Even though traditional soil characterization provides soil information by horizon, proximal soil sensors will be able to provide continuous information about soil properties with depth. Overall, not averaging the spectra by soil horizon before putting the data into a PLS calibration is more practical and preferred as not averaging provides a greater resolution of soil characteristics with depth.

3) What is the gain in prediction accuracy by boosting an in situ spectral library with local samples of the same soil series?

Construction of large regional and/or global libraries to increase VisNIR-DRS predictability has been promoted (Brown et al., 2005; Shepherd et al., 2002) and now VisNIR-DRS is one of the cornerstone methods used in the GlobalSoilMap.net project

(Sanchez et al., 2009). Studies have addressed creating a global spectral library robust enough to predict soil properties from a wide range of soils (Shepherd et al., 2002; Brown et al., 2005; Brown et al., 2007; Sankey et al., 2008; Minasny et al., 2009). One study created a small intact, whole-profile spectral library (Waiser et al., 2007; Morgan et al., 2009).

Results of this study indicate that using an in situ spectral library boosted with local samples is a preferable method for characterizing properties of soil cores. The Central Texas library boosted with Field 100 had the best predictions. However, Field 200 alone predicted clay content better than the Central Texas data boosted with Field 200. The principal component plots show that Field 100 and the Central Texas data soils are spectrally similar, while Field 200 soils have similar and dissimilar spectral features. Field 200 predicted clay content of Field 100 best because it overlaps more spectral points of Field 100 (Fig. 4.4). Prediction accuracy was improved when the Central Texas data were boosted with Field 100, but did not improve when boosted with Field 200. When creating calibration libraries, it is useful to look at the spectral similarities (e.g. principal components) of the calibration and validation data. Global libraries do not work alone because soils are from different parent materials and because of the various lab techniques performed to calibrate the models; therefore, boosting a global library with a few local samples provides more efficient and costly predictions than collecting many local samples for calibration (Sankey et al., 2008).

4) How do quantitative predictions of soil properties and categorical classification of VisNIR-DRS data compare when classifying soil to series?

Wilson and Davilla are very similar soil series that are hard even for the NRCS personnel to distinguish, because mapping soil series is subjective and protocol can be different depending on the site. Soil scientists rely on previous knowledge of landscape and soil positions to help map soil series. The soil cores used in this study were classified three different times, first, by the soil survey map, then in the field by a NRCS soil scientist, and finally adjusted according to the laboratory characterization information. It is difficult for someone without expertise to distinguish between the Wilson and Davilla series, even using PLS. Using LDA to predict the soil series provides a direct method that would eliminate guided classification.

In general, all the semi-independently calibrated models (PLS, LDA, and PLS plus LDA) performed better than the full-independently calibrated models. Using the semi-independent PLS-only and LDA plus PLS models, all soil cores were correctly classified into their NRCS soil series. Performing semi-independent LDA with the same spectral data as the semi-independent PLS models did not work as well at predicting soil series. Semi-independent models will always perform better, but it is important to include fully-independent models to more correctly assess the performance of VisNIR-DRS.

As expected, using the fully-independent PLS-only model instead of the semi-independent models decreased the classification accuracy by 55 and 81 % for Fields 100 and 200, respectively, with a kappa coefficient of 0.50. Even though both fields had the

same soil series, prediction accuracy of fully-independent models can be affected because of different ranges of soil properties, depth to parent material, location, and moisture content. Even though PLS had classification accuracy comparable to unguided LDA, knowledge of pedology and how soil series are classified is needed when using PLS models to predict soil series.

Using LDA to directly classify soil series requires less expertise because the method bypasses the step of creating calibration models and the pedology knowledge is not needed to calculate texture and particle size class. Classifying series with LDA is very rapid and simple and requires no previous lab analysis (Pavon et al., 2003). Series may not be accurately predicted with LDA if the series are not well separated and overlap in the spectral data (Pontes et al., 2009). As seen in the principal components plots, Wilson, Davilla, and Burleson did not have distinct separation. Better predictions may also be made if outliers are removed after examining the principal components plots (Christy et al., 2008). Though the unguided LDA approach performed comparably to PLS, as with any hands-off approach, caution is advised.

Predicting soil series with the fully-independent LDA plus PLS produced poorer prediction accuracy than the fully-independent LDA models, with 52 % of the soil cores correctly classified. The first three principal components with respect to soil horizons A and B show some differentiation by horizons, particularly in the first two principal components (Fig. 4.6). Even though the horizons were spectrally different, LDA was not able to directly predict the horizons any better than series. Using LDA plus PLS is not practical because it requires as much guidance as PLS, without better results. Even

though PLS and LDA are using the same spectral data, overall PLS performed better for predicting soil series. This could be because too many variables may be causing the LDA models to overfit (Jain and Chandrasekaran, 1982). By selecting specific spectral bands for the model, classification may be improved.

CHAPTER VI

CONCLUSIONS

To achieve the ultimate goal of developing a multi-sensor platform for mapping soils, VisNIR-DRS methodologies for mapping soil profiles in the field need to be better defined. The goal of this research was to determine how VisNIR-DRS scans of soil cores can be used to identify soil properties, horizons, and classification at the soil series level, while using soil EC_a to help define the VisNIR-DRS soil sampling strategy. More specifically, this research addressed the following questions: 1) When scanning intact soil cores, is prediction accuracy of soil properties affected by whether the soil profiles are uniformly moist (field capacity) or variable (during natural wetting or drying phases); 2) How is prediction accuracy of soil properties affected by combining the same lab-measured clay content based on horizons with individual, 2.5-cm thick soil scans; 3) What is the gain in prediction accuracy by boosting an in situ spectral library with local samples of the same soil series; and 4) How do quantitative predictions of soil properties and categorical classification of VisNIR-DRS data compare when classifying soil profiles at the soil series level?

Overall VisNIR-DRS continues to demonstrate effectiveness for characterizing soil properties and classifying soil series on intact soil profiles. Study results indicate that wetting soils to uniform moisture prior to scanning improves prediction accuracy of total clay and sand contents. Estimates of prediction accuracy are affected depending on how spectral data are combined for both calibration and prediction. Even though improvements in prediction accuracy are minimal, it may be beneficial to collect two

sets of scans of an individual profile for averaging. The best prediction accuracy is seen when predicted clay content is averaged by horizon, however averaging the spectra or predicted clay contents by horizon is not practical because horizon depths may not be known and depth specific information is lost. When creating calibration models, boosting a library with local samples can improve prediction accuracy, and principal components plots provide insight on spectral similarities among data sets. Overall using fully-independent PLS alone performed the same as fully-independent LDA at predicting soil series. Most importantly, results of this project reiterate the importance of fully-independent calibration and validation for assessing the true potential of VisNIR-DRS.

To enhance future research using VisNIR-DRS for characterizing soils in the field, larger regional and global libraries need to be constructed. These libraries need to include spectral scans of intact soils and whole profiles because field mapping need calibration models based on intact cores. Methodologies for calculating the minimum number of local samples required for boosting the prediction accuracy of a spectral library need to be developed. To increase prediction accuracy using spectral libraries, selection techniques using principal components analysis, Mahalanobis distance, and other multivariate tools need to be investigated. Overall VisNIR-DRS is an effective way for characterizing properties and classifying soil series as part of a multi-sensor platform.

REFERENCES

Abdu, H., D.A. Robinson, and S.B. Jones. 2007. Comparing bulk soil electrical conductivity determination using the DUALEM-1S and EM38-DD electromagnetic induction instruments. Soil Sci. Soc. Am. J. 71:189–196.

Ben-Dor, E., D. Heller, and A. Chudnovsky. 2008. A novel method of classifying soil profiles in the field using optical means. Soil Sci. Soc. Am. J. 72:1113-1123.

Bricklemeyer, R.S., and D.J. Brown. 2010. On-the-go VisNIR: Potential and limitations for mapping soil clay and organic carbon. Compt. Electron. Agric. 70:209-216.

Brown, D.J. 2007. Using a global VNIR soil-spectral library for local soil characterization and landscape modeling in a 2nd order Uganda watershed. Geoderma 140:444-453.

Brown, D.J., R.S. Bricklemeyer, and P.R. Miller. 2005. Validation requirements for diffuse reflectance soil characterization models with a case study of VNIR soil C prediction in Montana. Geoderma. 129:251-267.

Brown, D.J., K.D. Shepherd, G. Walsh, M.D. Mays, and T.G. Reinsch. 2006. Global soil characterization with VNIR diffuse reflectance spectroscopy. Geoderma 132:273-290.

Callegary, J.B., T.P.A. Ferré, and R.W. Groom. 2007. Vertical spatial sensitivity and exploration depth of low-induction-number electromagnetic-induction instruments. Vadose Zone J. 6:158–167.

Carrol, Z.L., and M.A. Oliver. 2005. Exploring the spatial relations between soil physical properties and apparent electrical conductivity. Compt. Electron. Agric. 128:354-374.

Chang, C.W., D.A. Laird, M.J. Maushbach, and C.R. Hurburgh, Jr. 2001. Near-infrared reflectance spectroscopy-principal components analyses of soil properties. Soil Sci. Soc. Am. J. 65:480-490.

Chang, C.W., and D.A. Laird. 2002. Near-infrared reflectance spectroscopic analysis of soil C and N. Soil Sci. 167:110-116.

Christy, C.D. 2008. Real-time measurement of soil attributes using on-the-go near infrared reflectance spectroscopy. Comput. Electron. Agric. 61:10–19.

Clark, R.N. 1999. Spectroscopy of rocks and minerals, and principals of spectroscopy. p. 3-52. *In* A.N. Rencz (ed.) Remote sensing for the earth sciences: Manual of remote sensing. John Wiley & Sons, New York.

Clark, R.N., T.V.V. King, M. Klejwa, and G.A. Swaze. 1990. High spectral resolution reflectance spectroscopy of minerals. J. Geophys. Res. 95:12653–12680.

Corwin D.L., and S.M. Lesch. 2005. Characterizing soil spatial variability with apparent soil electrical conductivity I. Survey protocols. Compt. Electron. Agric. 46:103-133.

Corwin D.L., and R.E. Plant. 2005. Applications of apparent electrical conductivity in precision agriculture. Compt. Electron. Agric. 46:1-10.

Doolittle, J.A., K.A. Sudduth, N.R. Kitchen, and S.J. Indorante. 1994. Estimating depths to claypans using electromagnetic induction methods. J. Soil Water Conserv. 49:572–575.

Dunn, B.W., H.G. Beecher, G.D. Batten, and S. Ciavarella. 2002. The potential of near-infrared reflectance spectroscopy for soil analysis – A case study from the Riverine Plain of south-eastern Australia. Aust. J. Exp. Agric. 42:607-614.

Gaffey, S.J. 1986. Spectral reflectance of calcite minerals in the visible and near infrared (0.35-2.55 microns): calcite, aragonite, and dolomite. Am. Mineral. 71:151-162.

Gauch, H.G., Jr., J.T.G. Hwang, and G.W. Fick. 2003. Model evaluation by comparison of model-based predictions and measured values. Agron. J. 95:1442-1446.

Goetz, A.F., S. Chabrillat, and Z. Lu. 2001. Field reflectance spectroscopy for detection of swelling clays at construction sites. Field Anal. Chem. Technol. 5:143-155.

Gower, J.C., and D.J. Hand. 1996. Biplots. Chapman and Hall, London, UK.

Hendrickx, J.M.H., B. Baerends, M. Sadig, and M.A. Chaudhry. 1992. Soil salinity assessment by electromagnetic induction of irrigated land. Soil Sci. Am. J. 56:1933-1941.

Hunt, G.R., and J.W. Salisbury. 1970. Visible and near-infrared spectra of minerals and rocks: I. Silicate minerals. Modern Geol. 1:283-300.

Islam, K., A. McBratney, and B. Singh. 2005. Rapid estimation of soil variability from the convex hull biplot of topsoil ultra-violet, visible, and near-infrared reflectance spectra. Geoderma 128:249-257.

Islam, K., B. Singh, and A. McBratney. 2003. Simultaneous estimation of several soil properties by ultra-violet, visible, and near-infrared reflectance spectroscopy. Aust. J. Soil Res. 41:1101-1114.

Jain, A.K., and B. Chandrasekaran. 1982. Dimensionality and sample size consideration in pattern recognition practice. p. 835-855. *In* (ed.) Handbook of Statistics. P.R. Krishnaiah and L.N. Kanal, The Netherlands.

Johnson, C.K., K.M. Eskridge, and D.L. Corwin. 2005. Apparent soil electrical conductivity: applications for designing and evaluating field-scale experiments. Comput. Electron. Agric. 46:181-202.

Kachanoski, R.G., E.G. Gregorich, and I.J. Van Wesenbeek. 1988. Estimating spatial variations of soil water content using non-contact in electromagnetic inductive methods. Can. J. Soil Sci. 68:715-722.

Khakural, B.R., P.C. Roberts, and D.R. Hugins. 1998. Use of non-contacting electromagnetic inductive methods for estimating soil moisture across a landscape. Commun. Soil Sci. Plant Anal. 29:2055–2065.

Kilmer, V.H., and L.Z. Alexander. 1949. Methods for making mechanical analyses of soil. Soil Sci. Am. J. 68:15-24.

Lagacherie, P. F., Baret, J.B. Feret, J.M. Netto, J.M. Robbez-Masson. 2008. Estimation of soil clay and calcium carbonate using laboratory, field and airborne hyper spectral measurements. Remote Sens. Environ. 112:825–835.

Lesch, S.M., J.D. Rhoades, L.J. Lund, and D.L. Corwin. 1992. Mapping soil salinity using calibrated electromagnetic measurements. Soil Sci. Soc. Am. J. 56:540-548.

Malley, D.F., L. Yesmin, and R.G. Eilers. 2002. Rapid analysis of hog manure and manure-amended soils using near-infrared spectroscopy. Soil Sci. Soc. Am. J. 66:1677-1686.

Martinez, A.M., and C.K. Avinash. 2001. PCA versus LDA. IEEE Trans. Patt. Anal. Mach. Intel. 23:228-233.

McCarty, G.W., L.B. Reeves, V.B. Reeves, R.F. Follett, and J.M. Kimble. 2002. Mid-infrared and near-infrared diffuse reflectance spectroscopy for soil C measurement. Soil Sci. Soc. Am. J. 66:640–646.

McNeill, J.D. 1980. Electrical conductivity of soils and rocks. Tech Note TN5. Geonics, Ltd., Mississauga, Ontario, Canada.

Mertens, F.M., S. Paetzold, and G. Welp. 2008. Spatial heterogeneity of soil properties and its mapping with apparent electrical conductivity. J. Plant. Nutr. 171:146-154.

Minasny, B., and A.B. McBratney. 2008. Regression rules as a tool for predicting soil properties from infrared reflectance spectroscopy. Chemometr. Intell. Lab. 94:72-79.

Minasny, B., A.B. McBratney, L. Pichon, W. Sun, and M.G. Short. 2009. Evaluating near infrared spectroscopy for field prediction of soil properties. Aust. J. Soil Res. 47:664-673.

Morgan, C.L., T.H. Waiser, D.J. Brown, and C.T. Hallmark. 2009. Simulated in situ characterization of soil organic and inorganic carbon with visible near-infrared diffuse reflectance spectroscopy. Geoderma 151:249-256.

Nelson, D.W., and L.E. Sommers, 1982. Total C, organic C, and organic matter. p. 539–580. *In* A.L. Page, (ed), Methods of soil analysis. Part II, ASA, SSSA, Madison, WI.

Pavon, J.L.P., M.D. Sanchez, C.G. Pinto, M.E.F. Laespada, B.M. Cordero, and A.G. Pena. 2003. A method for the detection of hydrocarbon pollution in soils by headspace mass spectrometry and pattern recognition techniques. Anal. Chem. 75:2034-2041.

Pontes, M.J.C., J. Cortez, R.K.H. Galvao, C. Pasquini, M.C.U Araujo, R.M. Coelho, M.K. Chiba, M.F. de Abreu, and B.E. Madari. 2009. Classification of Brazilian soils by using LIBS and variable selection in the wavelet domain. Anal. Chim. Acta. 642:12-18.

R Development Core Team. 2004. R: A language and environment for statistical computing. R Foundation for Statistical Computing. Vienna, Austria. Available: http://www.R-project.org.

Rhoades, J.D., and D.L. Corwin. 1981. Determining soil electrical conductivity–depth relations using an inductive electromagnetic soil conductivity meter. Soil Sci. Soc. Am. J. 45:2552–2560.

Rhoades, J.D., N.A. Manteghi, P.J. Shouse, and W.J. Alves. 1989. Soil electrical conductivity and soil salinity: new formulations and calibrations. Soil Sci. Soc. Am. J. 53:433–439.

Rhoades, J.D., P.A.C. Raats, and R.J. Prather. 1976. Effects of liquid-phase electrical conductivity, water content, and surface conductivity on bulk soil electrical conductivity. Soil Sci. Soc. Am. J. 40:651-655.

Sanchez, P.A., S. Ahamed, F. Carré, A.E. Hartemink, J. Hempel, J. Huising, P. Lagacherie, A.B. McBratney, N.J. McKenzie, M.L. Mendonça-Santos, B. Minasny, L. Montanarella, P. Okoth, C.A. Palm, J.D. Sachs, K.D. Shepherd, T. Vågen, B. Vanlauwe, M.G. Walsh, L.A. Winowiecki, G. Zhang. 2009. Digital soil map of the world. Science 325:680-681

Sankey J.B., D.J. Brown, M.L. Bernard, and R.L. Lawrence. 2008. Comparing local vs. global visible and near-infrared (VisNIR) diffuse reflectance spectroscopy (DRS) calibrations for the prediction of soil clay, organic C and inorganic C. Geoderma 148:149-158.

Sheets, K.R., and J.M.H. Hendrikx. 1995. Noninvasive soil water content measurement using electromagnetic induction. Water Resour. Res. 31:2401-2409.

Shepherd, K.D., and M.G. Walsh. 2002. Development of reflectance spectral libraries for characterization of soil properties. Soil Sci. Soc. Am. J. 66:988-998.

Sherrod, L.A., G. Dunn, G.A. Peterson, and R.L. Kolberg. 2002. Inorganic C analysis by modified pressure-calcimeter method. Soil Sci. Soc. Am. J. 66:299-305.

Steele, J.G., and R. Bradfield. 1934. The significance of size distribution in the clay fraction. Bull. Am. Soil Surv. Assoc. 15:88-93.

Sudduth, K.A., D.F. Hughes, and S.T. Drummond. 1995. Electromagnetic induction sensing as an indicator of productivity on claypan soils. p. 671–681. *In* P.C. Robert, R.H. Rust, and W.E. Larson (ed.) Site-specific management for agricultural systems. Proc. Int. Conf., 2nd, Minneapolis, MN. 27–30 Mar. 1994. ASA, CSSA, and SSSA, Madison, WI.

Soil Survey Staff. 1996. Soil survey laboratory methods and procedures for collecting soil samples. Soil survey investigations report no. 1. U.S. Gov. Print. Office, Washington, DC.

Soil Survey Staff. 2008. United States Department of Agriculture. NRCS. Web Soil Survey.

Viscarra-Rossel, R.A., S.R. Cattle, A. Ortega, and Y. Foua. 2009. In situ measurements of soil colour, mineral composition and clay content by Vis-NIR spectroscopy. Geoderma 150:253-266.

Viscarra-Rossel, R.A.V., D.J.J. Walvort, A.B. McBratney, L.J., Janik, and J.O. Skjemstad. 2006. Visible, near infrared, mid infrared or combined diffuse reflectance spectroscopy for simultaneous assessment of various soil properties. Geoderma 131:59-75.

Vitharana, U.W.A., T. Saey, L. Cockx, D. Simpson, H. Vermeersch, M. Van Meirvenne. 2008. Upgrading a 1/20,000 soil map with an apparent electrical conductivity survey. Geoderma 148:107-112.

Waiser, T., C.L.S. Morgan, D.J. Brown, and C.T. Hallmark. 2007. In situ characterization of soil clay content with VNIR diffuse reflectance spectroscopy. Soil Sci. Soc. Am. J. 71:389-396.

APPENDIX A

WILSON SERIES

The Wilson series consists of very deep, moderately well drained, very slowly permeable soils that formed in alkaline clayey sediments. These soils are on nearly level to gently sloping stream terraces or terrace remnants on uplands. Slopes are mainly less than 1 percent but range from 0 to 5 percent.

TAXONOMIC CLASS: Fine, smectitic, thermic Oxyaquic Vertic Haplustalfs

TYPICAL PEDON: Wilson silt loam--cropland. (Colors are for moist soil unless otherwise stated.)

Ap--0 to 5 inches; very dark gray (10YR 3/1) silt loam, gray (10YR 5/1) dry; weak fine granular structure; massive when dry; very hard, firm, sticky and plastic; common fine roots; moderately acid; abrupt wavy boundary. (3 to 10 inches thick)

Bt--5 to 20 inches; very dark gray (10YR 3/1) silty clay, gray (10YR 5/1) dry; moderate medium angular blocky structure; extremely hard, very firm, very sticky and very plastic; few fine roots; few fine pores; thin continuous clay films 1/2 unit of value darker than interior of peds; vertical cracks 1/2 inch wide are filled with material from the Ap horizon; slightly acid; gradual wavy boundary. (10 to 20 inches thick)

Btssg1--20 to 32 inches; grayish brown (2.5Y 5/2) silty clay, light brownish gray (2.5Y 6/2) dry; moderate medium angular blocky structure; extremely hard, very firm, very

sticky and very plastic; few fine roots; few fine pores; few slickensides; few medium pressure faces; thin continuous clay films on surface of peds; vertical cracks 1/4 inch wide partly filled with material from above; few fine crystals of gypsum; few fine calcium carbonate concretions; slightly alkaline; diffuse wavy boundary.

Btssg2--32 to 65 inches; grayish brown (2.5Y 5/2) silty clay, light brownish gray (2.5Y 6/2) dry; weak coarse angular blocky structure; extremely hard, very firm, very sticky and very plastic; few fine roots; few fine pores; few slickensides; patchy clay films on surface of peds; common fine crystals of gypsum; few fine masses of calcium carbonate; slightly alkaline; gradual smooth boundary. (combined Btss subhorizons are 25 to 60 inches thick)

BCkss--65 to 80 inches; olive gray (5Y 5/2) silty clay, light gray (5Y 7/2) dry; weak coarse angular blocky structure; extremely hard, very firm, very sticky and very plastic; few fine roots; few fine pores; few slickensides;
few coarse masses of calcium carbonate; few small fragments of clay; very slightly effervescent; moderately alkaline.

TYPE LOCATION: Kaufman County, Texas; 4 miles southeast of the intersection of Texas Highway 34 and U. S. Highway 175 in Kaufman, 0.15 mile northeast and 0.2 mile southeast of intersection of county road and U. S. Highway 175, 150 feet southwest in field.

RANGE IN CHARACTERISTICS: Solum thickness ranges from 60 to more than 80 inches. The weighted average clay content of the upper 20 inches of the argillic horizon ranges from 35 to 50 percent. When dry, cracks at least 1/4 inch wide extend from the top of the argillic horizon through a thickness of 12 inches or more within the upper 50 inches of the soil. Slickensides and/or wedged-shaped aggregates and pressure faces range from few to common and begin at a depth of 14 to 26 inches. Linear extensibility is greater than 2.5 inches (6 cm) within 40 inches (100 cm) of the soil surface. COLE ranges from 0.07 to 0.10 in the upper 50 inches of the argillic horizon. The surface layer is variable in thickness with a series of micro crests and troughs in the Bt horizon that range from 4 to about 20 feet apart. Redoximorphic features are contemporary in the upper Bt1 horizon and are mainly relic in the lower part of the Bt horizon. The soil does not have aquic soil conditions in the upper 20 inches in most years.

The A horizon is less than 10 inches thick in more than 50 percent of the pedon, but it is as much as 15 inches thick in some subsoil troughs. It has hue of 10YR or 2.5Y, value of 3 to 5, and chroma of 1 or 2. Texture is loam, silt loam, silty clay loam, clay loam or their gravelly counterparts. Siliceous pebbles and small cobbles range from 0 to 35 percent. It is massive and hard or very hard when dry but is soft or friable with structure when moist. Some pedons have a thin E horizon in subsoil troughs. Reaction ranges from moderately acid to neutral.

The Bt horizon has hue of 10YR or 2.5Y, value of 2 to 4, and chroma of 1 or less. Texture is clay loam, silty clay loam, silty clay, or clay. Some pedons have iron

concentrations in shades of brown or yellow that range from few to common. Siliceous pebbles range from 0 to about 15 percent by
volume. Reaction ranges from slightly acid to slightly alkaline.

The Btss horizon has hue of 10YR to 5Y, value of 3 to 7, and chroma of 2 or less. Iron concentrations in shades of yellow, brown or olive range from none to common. Texture is commonly silty clay or clay and less commonly silty clay loam or clay loam. Reaction ranges from moderately acid to slightly alkaline and is typically noncalcareous.

The BCk or BC horizon has colors in shades of gray or brown. Redoximorphic features of these colors and in other shades of yellow, red or olive range from few to many. Texture is clay loam, silty clay loam, silty clay, or clay. Some pedons have fragments or thin strata of shale or marl. These materials make up less than 35 percent of the matrix. Reaction ranges from neutral to moderately alkaline. Concretions and masses of calcium carbonate range from none to common.

The C horizon, where encountered, is shale or marl or stratified layers of shale, marl and clay.

COMPETING SERIES: There are no competing series. Similar soils are
the Dacosta, Herty, Lufkin, Mabank, and Steedham series. Dacosta soils have a mollic epipedon and are members of the hyperthermic family. Herty, Lufkin and Mabank soils have an abrupt texture change between the A and Bt horizon. In addition, Herty soils are

in the udic moisture regime. Steedham soils have sola from 20 to 40 inches thick, and are well drained.

GEOGRAPHIC SETTING: Wilson soils are on nearly level to gently sloping terraces or remnants of terraces. Slope gradients are 0 to 5 percent but dominantly less than 1 percent. The soil formed in alkaline clayey alluvium. Mean annual temperature ranges from 64 to 70 degrees F., and mean
annual precipitation ranges from 32 to 45 inches. Frost free days range from 220 to 270 days and elevation ranges from 250 to 700 feet. Thornthwaite P-E indices from 50 to 70.

GEOGRAPHICALLY ASSOCIATED SOILS: These are
the Bonham, Burleson, Crockett, Houston Black, Lufkin, Mabank,
and Normangee series. Bonham soils have mollic epipedons. Burleson soils are on similar positions. Burleson and
Houston Black soils are clayey to the surface and have slickensides (Vertisols). Crockett and Normangee soils have Bt horizons with chroma of more than 2. Bonham, Houston Black, Crockett and Normangee soils are on slightly higher positions above Wilson. Lufkin soils are on similar or
slightly lower concave positions. Mabank soils are on similar positions.

DRAINAGE AND PERMEABILITY: Moderately well drained. Permeability is very slow. Runoff is low on 0 to 1 percent slopes, medium on 1 to 3 percent slopes, and high on 3 to 5 percent slopes. Very slow internal drainage. The soil is seasonally wet and is

saturated in the surface layer and upper part of the Bt horizon during the winter and spring seasons for periods of 10 to 30 days.

USE AND VEGETATION: Wilson soils are cropped to cotton, sorghums, small grain, and corn. Many areas are now idle or are used for unimproved pasture. Original vegetation was tall prairie grasses, mainly andropogon species, and widely spaced motts of elm and oak trees. Most areas that are not cropped have few to many mesquite trees.

DISTRIBUTION AND EXTENT: Mainly in the Blackland Prairies of Texas, with small areas in Oklahoma. The soil is extensive, probably exceeding 1,000,000 acres.

MLRA OFFICE RESPONSIBLE: Temple, Texas

SERIES ESTABLISHED: Wilson County, Texas; 1907.

REMARKS: Classification change from Udertic Haplustalfs to Oxyaquic Vertic Haplustalfs based on knowledge that these soils are saturated for 2 to 4 weeks in most years. This period of time is within the definition of saturation for one month or more if rules of rounding are applied, i.e., 2 to 6 weeks saturation is considered inclusive.

Diagnostic horizons and features recognized in this pedon are:

Ochric epipedon - 0 to 5 inches. (A horizon; very hard and massive when dry).

Argillic horizon - 5 to 65 inches. (Bt horizons)

Vertic feature - Cracks in the upper part of the argillic horizon (5 to 32 inches), few slickensides between 20 and 77 inches, and linear extensibility greater than 6.0 cm.

ADDITIONAL DATA: Type location pedon NSSL S62TX-(129)257-2 Kaufman County, Texas. Texas Ag. Exp. Station Lab. S63TX-145-1; S82TX-289-32

DAVILLA SERIES

The Davilla series consists of very deep, moderately well drained, very slowly permeable soils on Pleistocene Age terraces. These nearly level soils formed in loamy and clayey sediments. Slopes range from 0 to 2 percent.

TAXONOMIC CLASS: Fine-loamy, siliceous, superactive, thermic Udic Haplustalfs

TYPICAL PEDON: Davilla loam--in an area of Wilson-Davilla complex on a 0.5 percent convex slope in a idle cropland field. (Colors are for dry soil unless otherwise stated.)

Ap--O to 10 inches; dark brown (7.5YR 4/3) loam, dark brown (7.5YR 3/4) moist; weak fine granular structure when moist, massive when dry; very hard, friable; few fine roots; few wormcasts; few siliceous pebbles up to 1 cm in diameter; slightly acid; clear wavy boundary. (6 to 18 inches thick)

Bt1--10 to 24 inches; brown (10YR 5/3) clay loam, dark brown (1OYR 4/3) moist; weak fine and medium angular blocky structure; very hard, firm; few fine roots; few fine pores; few wormcasts; few fine distinct light gray (10YR 7/1) and brownish yellow (10YR 6/6) redoximorphic features with sharp boundaries; few thin clay films on surfaces of peds; few fine iron-manganese concretions; few siliceous pebbles up to 5 mm in diameter; neutral; gradual wavy boundary.

Bt2--24 to 34 inches; brown (1OYR 5/3) clay loam, dark brown (1OYR 4/3) moist; weak medium angular blocky structure; very hard, firm; few fine roots; few fine pores;

common fine distinct light gray (10YR 7/1) and few fine prominent reddish yellow (5YR 6/6) redoximorphic features with sharp boundaries; few thin clay films on surfaces of peds; few fine iron-manganese concretions; few siliceous pebbles up to 5 mm in diameter; neutral; gradual wavy boundary. (combined Bt subhorizons are 18 to 70 inches thick)

Btg1--34 to 44 inches; light brownish gray (1OYR 6/2) clay loam, grayish brown (1OYR 5/2) moist; weak medium angular blocky structure; very hard, firm; few fine roots; few fine pores; common fine prominent reddish yellow (7.5YR 6/8) redox concentrations with sharp boundaries; few fine streaks and masses of light gray (10YR 7/1) albic material; few thin clay films on surfaces of peds; few fine iron-manganese concretions; few siliceous pebbles up to 5 mm in diameter; slightly alkaline; gradual wavy boundary.

Btg2--44 to 50 inches; light gray (1OYR 6/1) clay loam, gray (10YR 5/1) moist; weak medium angular blocky structure; extremely hard, very firm; common fine distinct brownish yellow (10YR 6/6) redox concentrations with sharp boundaries; few fine iron manganese concretions; few thin clay films; few siliceous pebbles up to 5 mm in diameter; slightly alkaline; gradual wavy boundary.

Btg3--50 to 60 inches; light gray (10YR 6/1) clay loam, gray (1OYR 5/1) moist; weak medium angular blocky structure; extremely hard, very firm; few fine distinct brownish yellow (10YR 6/6) redox concentrations with sharp boundaries; few patchy clay films;

few fine iron-manganese concretions; few fine concretions of calcium carbonate; few siliceous pebbles up to 5 mm in diameter; slightly alkaline; gradual wavy boundary.

Btg4--60 to 80 inches; light gray (1OYR 7/1) clay loam; light gray (10YR 6/1) moist; weak medium angular blocky structure; extremely hard, very firm; few fine faint brownish yellow (10YR 6/8) redox concentrations with clear boundaries; few fine iron-manganese concretions; few fine concretions of calcium carbonate; few patchy clay films; few siliceous pebbles up to 5 mm in diameter; slightly alkaline. (combined Btg subhorizons are 0 to 46 inches thick)

TYPE LOCATION: Milam County, Texas; from junction of Farm Road 487 and Farm Road 437 in Davilla approximately 3.6 miles southeast on Farm Road 487, approximately 50 feet north into brushy rangeland north of road.

RANGE IN CHARACTERISTICS: Solum thickness is more than 80 inches. The weighted average clay content of the control section ranges from 27 to 35 percent. Redoximorphic features, which are masses, are considered to be mainly relic features. During wet years these soils may be saturated long enough to develop aquic soil conditions in some subhorizons. However, in most years they do not have aquic soil conditions. A few siliceous pebbles and/or rounded ironstone pebbles are on the surface and in some subhorizons of most pedons.

The A horizon ranges from 6 to 18 inches thick. It has hue of 7.5YR or 1OYR, value of 4 to 6, and chroma of 2 to 4. Texture is very fine sandy loam or loam. Reaction is slightly acid or neutral.

The Bt horizon has hue of 7.5YR, 1OYR or 2.5Y, value of 4 to 7, and chroma of 2 to 6. Redoximorphic features in shades of red, gray, brown, or yellow range from few to common. Texture is sandy clay loam or clay loam. Reaction ranges from slightly acid to slightly alkaline.

The Btg or lower Bt horizon has matrix colors in shades of gray, brown, yellow, or olive. Redoximorphic features in shades of red, gray, yellow, or brown range from few to many. Texture is sandy clay loam, clay loam, or clay. Concretions and soft masses of calcium carbonate range from none to few. Reaction ranges from slightly acid to moderately alkaline. Most pedons are underlain with beds of sand and/or gravel below a depth of 10 feet.

COMPETING SERIES: These are the Gholson, Lavender, May, and Personville series in the same family and the similar Bremond, Chazos, Gredge, Minerva, and Rader series. Gholson and Minerva soils have and argillic horizon with hue redder than 7.5YR. Lavender and Personville soils have a lithic contact of limestone within 60 inches of the surface. May soils have a mollic colored epipedon. Bremond, Chazos, and Gredge soils have a fine particle-size control section.

GEOGRAPHIC SETTING: Davilla soils are on nearly level terraces of Pleistocene age. These soils formed mainly in loamy sediments. The surface is typically mounded. The mounds are oval and range from 20 to about 80 feet in diameter. They are about 6 to 18 inches above the associated intermound areas except where cultivation has smoothed and leveled the surface. Davilla soils are on the mounds. They are typically mapped in a complex with another soil. Slope gradients range from 0 to 2 percent. The climate is subhumid with an average precipitation of 32 to 40 inches. The mean average temperature is 66 to 69 degrees F. Frost free days range from 250 to 275. The elevation ranges from 300 to 500 feet above sea level. Thornthwaite P-E indices range from 54 to 64.

GEOGRAPHICALLY ASSOCIATED SOILS: These include
the Benchley, Chazos, Crockett, Edge, Gause, Gredge, Luling, and Wilson soils. The Benchley, Crockett, Edge, and Luling soils have a solum that is underlain by geologic materials within a depth of 60 inches and they have fine textured control sections. They are slightly higher in the landscape and are on nearby uplands. The Chazos, Gause, Gredge, and Wilson soils are on similar terrace positions. These soils have fine textured control sections. In addition Chazos and Gause soils have a loamy fine sand epipedon. Gredge soils have an argillic horizon with reddish matrix colors. Wilson soils have a very dark gray upper argillic horizon and are mapped in complex with Divalla. They are commonly in the slightly lower intermound position.

DRAINAGE AND PERMEABILITY: Moderately well drained and the permeability is very slow. Runoff is medium.

USE AND VEGETATION: These soils are used mainly for improved pasture with coastal bermudagrass and bahiagrass being the dominant grasses grown. Some areas are cropped to small grains, corn, or grain sorghum. Some areas are in rangeland. Native vegetation consists of medium and tall grasses with scattered elm, hackberry, mesquite and post oak trees.

DISTRIBUTION AND EXTENT: Mainly in central Texas. In MLRA 86A, 86B and 87A. The series is of moderate extent.

MLRA OFFICE RESPONSIBLE: Temple, Texas

SERIES ESTABLISHED: Milam County, Texas; 1988.

REMARKS: Classification changed (2/94) from Aquic subgroup to Udic subgroup based on changes in aquic soil definitions and moisture data from similar soils. These soils were previously included with the Crockett series.

The diagnostic horizons and features recognized in this pedon are:

Ochric epipedon - from 0 to 10 inches (Ap horizon). The soil is massive and very hard when dry.

Argillic horizon - from a depth of 10 to 80 inches (Bt and and Btg horizons).

ADDITIONAL DATA: Data from 4 pedons shows the weighted average clay content of the control section ranges from 28 to 34 percent. However, the field texture method suggests a fine family.

BURLESON SERIES

The Burleson series consists of very deep, moderately well drained, very slowly permeable soils that formed in alkaline clayey sediments. These soils are on nearly level to gently sloping Pleistocene terraces. Slopes range from 0 to 5 percent.

TAXONOMIC CLASS: Fine, smectitic, thermic Udic Haplusterts

TYPICAL PEDON: Burleson clay--native pasture; in a pit midway between center of microdepression and microknoll. (Colors are for moist soil unless otherwise stated).

A1--0 to 6 inches; black (10YR 2/1) clay, very dark gray (10YR 3/1) dry; moderate medium subangular blocky structure parting to moderate very fine angular blocky; very hard, very firm, very sticky and very plastic; many fine roots; cracks from 1/2 to 1 1/2 inches wide extend through the horizon; few snail shell fragments; few fine siliceous pebbles; slightly alkaline; gradual smooth boundary. (4 to 12 inches thick)

A2--6 to 12 inches; black (10YR 2/1) clay, very dark gray (10YR 3/1) dry; moderate medium angular blocky structure parting to moderate very fine angular blocky; very hard, very firm, very sticky and very plastic; many fine roots; cracks from 1/2 to 1 1/2 inches wide extend through the horizon; common distinct pressure faces; few fine siliceous pebbles; slightly alkaline. (0 to 12 inches thick)

Bss1--12 to 24 inches; very dark gray (10YR 3/1) clay; moderate medium and coarse angular blocky structure; few wedge-shaped peds: very hard, very firm, very sticky and very plastic; few fine roots; many large grooved slickensides tilted from horizontal 30 to

60 degrees; few fine siliceous pebbles; few fine iron-manganese concretions and masses; moderately alkaline; gradual wavy boundary. (8 to 30 inches thick)

Bss2--24 to 39 inches; very dark gray (10YR 3/1) clay; moderate medium and coarse angular blocky structure; common wedge-shaped peds: very hard, very firm, very sticky and very plastic; few fine roots; cracks from 1/2 to 1 inch wide extend through the horizon; many large grooved slickensides tilted from horizontal 30 to 60 degrees; few fine iron-manganese concretions and masses; few fine concretions and masses of calcium carbonate; few fine siliceous pebbles; very slightly effervescent; moderately alkaline; gradual wavy boundary. (8 to 30 inches thick)

Bss3--39 to 51 inches; dark gray (10YR 4/1) clay; few fine and medium streaks and spots of pink (5YR 7/4); moderate medium and coarse angular blocky structure; many wedge-shaped peds; very hard, very firm, very sticky and very plastic; few fine roots; many large grooved slickensides tilted from horizontal 30 to 60 degrees; few fine iron-manganese concretions and masses; few fine concretions of calcium carbonate; few fine siliceous pebbles; slightly effervescent; moderately alkaline; clear irregular boundary. (0 to 20 inches thick)

Bss4--51 to 76 inches; dark gray (10YR 4/1) clay; common reddish brown (5YR 4/3) streaks and spots of; moderate medium and coarse angular blocky structure; common wedge- shaped peds; very hard, very firm, very sticky and very plastic; few fine roots; many large grooved slickensides tilted from horizontal 30 to 60 degrees; few very dark

gray crack fillings; few iron-manganese concretions; few concretions and masses of calcium carbonate; slightly effervescent; moderately alkaline. (0 to 36 inches thick)

2BCkss--76 to 80 inches; yellowish red (5YR 4/6) silty clay; few streaks of light gray (10YR 6/1); moderate coarse angular blocky structure; common wedge shaped peds; very hard, very firm, very sticky and very plastic; few fine roots; many large grooved slickensides tilted from horizontal 30 to 60 degrees; few dark gray crack fillings; common concretions and masses of calcium carbonate; strongly effervescent; moderately alkaline.

TYPE LOCATION: Burleson County, Texas; from intersection of Farm Road 2155 and Farm Road 60 in northwest edge of Snook, Texas; 0.7 mile southwest on Farm Road 60; 220 feet south in native pasture. (Latitude: 30 degrees, 29 minutes, 18 seconds north; Longitude: 96 degrees, 28 minutes, 50 seconds west)

RANGE IN CHARACTERISTICS: The solum is 60 to more than 80 inches thick. The control section has 40 to 60 percent clay and more than 28 percent silt. Iron-manganese concretions and masses range from none to few throughout. This is a cyclic soil and undisturbed areas have gilgai microrelief with microknolls 6 to about 12 inches higher than microdepressions. Distance between the center of the microknoll and the center of the microdepression is about 5 to 15 feet. The microknoll makes up about 20 percent, the intermediate, or area between the knoll and depression, about 50 percent, and the micro depression about 30 percent. When dry, cracks 1 to 3 inches wide extend from the

surface to a depth of 40 inches or more. The cracks remain open for 90 to 150 cumulative days during most years. Slickensides begin at a depth of 8 to 24 inches.

The A horizon has hue of 10YR, value of 2 or 3, and chroma of 1 or less. Texture is clay, silty clay, or gravelly clay. Some pedons have loamy Ap horizons containing more than 35 percent clay. Gravelly layers are less than 20 inches thick and contain 15 to 35 percent siliceous pebbles. Reaction ranges from moderately acid to slightly alkaline. However, on microknolls some pedons are moderately alkaline.

The upper Bss horizons have hue of 10YR, value of 2 to 4 and chroma of 1 or less. Texture is silty clay or clay. Redoximorphic features range from none to few in shades of brown or gray. Siliceous pebbles range from none to few. Hard pitted concretions of calcium carbonate range from none to few. Reaction ranges from moderately acid to moderately alkaline and typically is noneffervescent.

The lower Bss or Bkss horizons have hue of 10YR to 5Y, value of 4 to 6, and chroma of 1 or 2. Matrix chroma of 2 are below a depth of 40 inches, if encountered. Redoximorphic features in shades of yellow, brown, or gray range from none to common. Streaks or spots in shades of pink or red range from none to common. Texture is silty clay or clay. Siliceous pebbles range from none to about 5 percent. Reaction is slightly alkaline or moderately alkaline. It ranges from noneffervescent to strongly effervescent. Concretions and masses of calcium carbonate range from none to common.

The 2BCkss horizon, or 2CBkss horizon where present, has colors in shades of red, yellow, pink, or brown. Texture is clay loam, silty clay loam, or silty clay. Siliceous pebbles range from none to about 5 percent. Concretions and masses of calcium carbonate range from few to many. The reaction is moderately alkaline and effervescence ranges from slight to violent. The 2C horizon is not present in all pedons. It is mainly in soils on the Brazos River terrace. Burleson soils on other terrace systems commonly have colors in shades of gray or brown. Texture is typically clay. Some pedons have sandy or loamy textures with or without strata of gravel below a depth of 80 inches and most pedons have these materials below a depth of 12 feet.

COMPETING SERIES: These include

the Bleiblerville, Branyon, Clarita, Dimebox, Ellis, Fairlie, Heiden, Houston Black, Leson, Luling, Ovan, Sanger, Slidell, Tamford, and Watonga series. Bleiblerville, Heiden, Houston Black, and Sanger soils are calcareous throughout, and have more amplitude of waviness. Branyon and Slidell soils are calcareous at depths of less than 12 inches in over half the pedon. Clarita soils have subsoils in hue of 7.5YR or redder. Ellis soils have sola less than 60 inches. Fairlie soils have a paralithic contact with chalk at a depth of 40 to 60 inches. Dimebox soils contain ironstone fragments in the surface layer, have more amplitude of waviness, and are on uplands. Leson soils have more amplitude of waviness and typically have chroma of 2 or more within 40 inches of the surface. Luling soils have chroma of 2 throughout and are on uplands. Ovan soils have chroma of 2 throughout and are on flood plains. Tamford soils have red or reddish brown C

horizons and have mean annual temperature less than 65 degrees F. Watonga soils have sola less than 60 inches thick and are on flood plains.

GEOGRAPHIC SETTING: Burleson soils are on stream terraces and Pleistocene Age terraces. These are associated mainly with upland soils. Slope gradients are mainly less than 2 percent, but range to 5 percent. The soil formed in alkaline, clayey, alluvial sediments. Mean annual precipitation ranges from 32 to 40 inches, and mean annual temperature ranges from about 65 to 70 degrees F. Frost free days range from 220 to 270, and elevation ranges from 300 to 800 feet. Thornthwaite annual P-E indices range from 48 to 68.

GEOGRAPHICALLY ASSOCIATED SOILS: These are the competing Heiden, Houston Black and Leson series and the Kaufman, Ships, and Wilson series. Kaufman and Ships soils have very-fine control sections, and Ships soils have hue redder than 10YR. Heiden, Houston Black, and Leson soils are on slightly higher uplands. Kaufman and Ships soils are on slightly lower flood plains. Wilson soils have argillic horizons, and are on similar positions.

DRAINAGE AND PERMEABILITY: Moderately well drained. Very slow permeability. Runoff is low on 0 to 1 percent slopes, medium on 1 to 3 percent slopes, and high on 3 to 5 percent slopes. Water enters the soil rapidly when it is dry and cracked, and very slowly when it is moist.

USE AND VEGETATION: Cultivated crops are mainly cotton, sorghum, corn and small grains. Areas in native rangeland produce little bluestem, big bluestem, Indiangrass, eastern gamma, and switchgrass in excellent condition. Pasture grasses include improved bermudagrass, common bermudagrass, and kleingrass.

DISTRIBUTION AND EXTENT: The Blackland Prairies of Texas (MLRA 86A and 86B). The series is extensive.

MLRA OFFICE RESPONSIBLE: Temple, Texas

SERIES ESTABLISHED: Brazos County, Texas; 1951.

REMARKS: Diagnostic horizons and features recognized in this pedon are:

Mollic epipedon - 0 to 39 inches (A1, A2, Bss1, Bss2).

Vertisol features: Deep wide cracks that are open 90 to 150 cumulative days.

Large slickensides below the A horizon and throughout the soil.

ADDITIONAL DATA: National Soil Survey Laboratory: S62TX-43-3(LSL17746-17752), S62TX-43-4(LSL17753-17759), S77TX-051-5(78P0039-78P0047), and S77TX-051-6(78P0048-78P0056).

VITA

Name:	Katrina Margarette (Hutchison) Wilke
Address:	Department of Soil and Crop Science 2474 TAMU, College Station, TX, 77845-2474
Email Address:	khutchison@ag.tamu.edu
Education:	B.S., Bioenvironmental Sciences, Texas A&M University, 2008 M.S., Soil Science, Texas A&M University, 2010